7-17-2008

Fate of Volatile Chemicals during Accretion on Wet-Growing Hail

Ryan A. Michael
University of South Florida

Fate of Volatile Chemicals during Accretion on Wet-Growing Hail

by

Ryan A. Michael

A thesis submitted in partial fulfillment
of the requirements for the degree of
Master of Science in Engineering Science
Department of Civil and Environmental Engineering
College of Engineering
University of South Florida

Major Professor: Amy L. Stuart, Ph.D.
Jeffrey Cunningham, Ph.D.
Jennifer M. Collins, Ph.D.
Maya A. Trotz, Ph.D.

Date of Approval:
July 17, 2008

Keywords: atmospheric chemistry, riming, retention, ice microphysics, cloud modeling

Acknowledgements

This thesis would not have been successfully completed without the help of many people to whom I am grateful and because of whom my experience has been unforgettable.

First, I wish to convey my thanks to my advisor, Amy Stuart, for making this feasible. From providing funds to instilling knowledge, your support throughout my study has been paramount to my success. Thank you for holding me to such high standards with your perceptive remarks and constructive criticisms at every stage of my research. More importantly, thank you for your patience, for sticking with me when even I wanted to throw my hands up.

I thank the members of my thesis committee, Maya Trotz, Jennifer Collins, and Jeffrey Cunningham. Thank you for your meticulous reviews. Your insightful comments were instrumental in helping to shape this work.

I am forever grateful to the late Calvin Miller who did not give me life but gave me the life I have. Thank you for believing in me, you are forever in my thoughts.

I would like to express my gratitude to the following persons for their help throughout this process: Chris Einmo, Monica Gray, Roland Okwen, Edolla Prince, Luis Baluto Torrez, and Nicole Watson

To my loving mother, Adnic West, to whom this thesis is dedicated, I say thank you. I am most indebted to you for your inestimable help, limitless sacrifices, and unconditional love throughout my life. Without you, this would not have been possible.

Table of Contents

List of Tables

List of Figures

Fate of Volatile Chemicals during Accretion on Wet-Growing Hail

Ryan Michael

ABSTRACT

Phase partitioning during freezing of hydrometeors affects the transport and distribution of volatile chemical species in convective clouds. Here, the development, evaluation, and application of a mechanistic model for the study and prediction of partitioning of volatile chemical during steady-state hailstone growth are discussed. The model estimates the fraction of a chemical species retained in a two-phase growing hailstone. It is based upon mass rate balances over water and solute for constant accretion under wet-growth conditions. Expressions for the calculation of model components, including the rates of super-cooled drop collection, shedding, evaporation, and hail growth were developed and implemented based on available cloud microphysics literature. A modified Monte Carlo simulation approach was applied to assess the impact of chemical, environmental, and hail specific input variables on the predicted retention ratio for six atmospherically relevant volatile chemical species, namely, SO_2, H_2O_2, NH_3, HNO_3, CH_2O, and HCOOH. Single input variables found to influence retention are the ice-liquid interface supercooling, the mass fraction liquid water content of the hail, and the chemical specific effective Henry's constant (and therefore pH). The fraction retained increased with increasing values of all these variables. Other single variables, such as hail

diameter, shape factor, and collection efficiency were found to have negligible effect on solute retention in the growing hail particle. The mean of separate ensemble simulations of retention ratios was observed to vary between 1.0×10^{-8} and 1, whilst the overall range for fixed values of individual input variables ranged from 9.0×10^{-7} to a high of 0.3. No single variable was found to control these extremes, but rather they are due to combinations of model input variables.

1. Introduction

1.1. Background

Knowledge of the upper tropospheric ozone budget is essential to our ability to understand and predict climate change. Ozone concentrations in the troposphere are regulated by catalytic cycles involving nitrogen oxides (NO_x), hydrogen oxides (HO_x), and volatile organic carbon (VOC) species. In upper tropospheric regions influenced by convection, the budget of NO_x and the ratio of HO_x to NO_y (reactive nitrogen) are not well understood, resulting in poorly understood ozone amounts [*Jaeglé et al.*, 2001].

1.2. Convective cloud systems

The availability and concentration of ozone precursors in the troposphere are significantly affected by the action of convective cloud systems. Convective cloud systems significantly influence tropospheric chemistry and chemical deposition to the ground by moving trace gas species from the boundary layer to the free troposphere through chemical scavenging by cloud hydrometeors. Convective processing of trace gas species is an important means of moving chemical constituents rapidly between the boundary layer and free troposphere, and is an effective way of cleansing the atmosphere through wet deposition. It also brings into the cloud, species that are of a different composition, concentration, and origin than the air that ascends from the boundary layer

[*Barth et al.*, 2002]. This entrained air can affect local thermodynamics as well as chemical and microphysical processes.

Convective cloud systems have been shown to influence the chemical characteristics of the upper troposphere to lower stratosphere region. They contribute to the production, transportation, and redistribution of reactive chemical constituents, including water, aerosols and long-lived tracers in the upper troposphere to lower stratosphere [*Dickerson et al.*, 1987; *Gimson*, 1997; *Lelieveld and Crutzen,* 1994; *Ridley et al.*, 2004; *Yin et al.*, 2005]. These convective cloud systems can offer a rapid pathway for the vertical transport of air containing reactive chemical species from the planetary boundary layer to the upper troposphere [*Barth et al.*, 2007; 2001]. Through entrainment/detrainment processes, they can facilitate the mixing and dispersal of pollutants, and the transport of reactive species over significantly shorter timescales than would occur via eddy diffusion or other atmospheric mixing processes [*Dickerson et al.*, 1987]. At higher altitudes, increases in wind speed may result in longer atmospheric residence times of chemical species, thus increasing the probability of their participation in photochemical reactions and other atmospheric transformations [*Ridley et al.*, 2004; *Stockwell et al.,* 1990; *Rutledge et al.*, 1986]. Thus, convective cloud systems can be thought of as chemical reactors, processing atmospheric air and its trace chemical constituents.

However, the potential cleansing effect of deep convective cloud systems on the atmospheric boundary layer is countered by negative impacts due to scavenging, dissolution, and eventual deposition of acidic species. Effects of acid deposition may include reduced buffering capacity of lakes and other surface water systems, forest

deaths, reduced visibility, material deterioration, and deleterious health effects such as bronchitis and asthma [*Cosby et al.*, 1985; *Likens et al.*, 1996; *Dockery et al*., 1996]. Furthermore, venting of air from the atmospheric boundary layer by convective cloud systems may influence tropospheric ozone concentrations due to the migration and increased residence times of chemical species that regulates its production. These processes may significantly affect the upper troposphere ozone budget, and consequently climate change [*Barth et al.*, 2002; *Dickerson et al*, 1987]. Additionally, as a result of these strong convective processes, regional air pollution problems may be transformed to global air pollution problems due to the long range transport of pollution plumes [*Dickerson et al*, 1987]. Therefore, an understanding of the microphysical processes governing the interaction of trace chemical species and condensed phase in convective cloud system is imperative to our determination of their fate, and as understanding of tropospheric ozone budget and climate change.

1.3. Cloud hydrometeors and chemical interactions

Previous studies have shown that the interaction of cloud hydrometeors with trace chemical species may significantly influence the fate of these chemicals, and subsequently impact atmospheric chemistry. Hydrometeors refer to the different forms of condensed water that constitute convective clouds, and include ice crystals, snow, graupel, and hail. Their formation is as a direct result of the moisture, temperatures, pressures, and airflow conditions associated with convective cloud systems. These cloud hydrometeors provide surfaces for chemical phase changes and reactions, act as condensed-phase reactors, and serve as conduits for chemical transport from the

atmosphere to the ground, through scavenging and precipitation [*Lamb and Blumenstein*, 1987; *Rutledge et al*, 1986; *Santachiara et al.*, 1995; *Snider and Huang*, 1998]. Interactions of volatile trace chemicals with cloud hydrometeors include absorption, condensation, diffusion, vapor deposition, or incorporation into the growing hydrometeor [*Flossmann et al,* 1985; 1987*; Pruppacher and Klett,* 1997]. Once dissolved in the hydrometeor, depending on the characteristics of the phase, the trace chemicals may dissociate or undergo further chemical reactions, thus affecting and modifying cloud and atmospheric chemical distributions [*Barth*, 2000; 2001; 2007]. For example, the removal of odd hydrogen species due to interactions with cloud hydrometeors has been found to significantly affect the oxidizing capacity of the troposphere and contribute to increased levels of sulfur species in precipitation [*Audiffren* et al, 1999; *Snider*, 1998]. Consequently, emphasis has been placed on understanding the interaction of trace chemical species with hydrometeors in convective cloud systems through observational and modeling studies. These include studies focusing on acid deposition [*Barth et al.*, 2000; *Chameides*, 1984; *Daum et al.*, 1984; *Kelly et al.*, 1985], ozone in the troposphere [*Lelieveld and Crutzen*, 1994; *Pickering et al.,* 1992; *Prather and Jacob*, 1997], and the interaction of hydrometeors with other species [*Chatfield* and *Crutzen* 1984]. Most of the models focused on liquid phase hydrometeors, and chemical species were distributed based on processes governing liquid-phase exchanges. Consequently, little is known about how microphysical processes involving ice affect chemical fate.

1.4. Ice-chemical interactions

Previous work indicates that ice-chemical interactions may have significant impacts on cloud and atmospheric chemistry [*Pruppacher and Klett*, 1997; *Stuart and Jacobson*, 2003; 2004; 2006]. Many researchers have included limited ice-chemical interactions in cloud models [*Audiffren et al*., 1999; *Chen and Lamb,* 1994; *Cho*, 1989; *Rutledge et al*., 1986]. *Audiffren et al.* [1999], in their two-dimensional Eulerian cloud model, utilized the formulations of *Lamb and Blumenstein* [1987] and *Iribarne and Barrie* [1950] in their parameterization of the entrapment of chemical species in a growing ice-phase hydrometeor. Elucidation of the mechanism by which trace chemicals and ice interact is important in order to predict chemical fate and to find suitable parameterizations for larger scale modeling.

Recent studies indicate that one microphysical process, the freezing of super-cooled drops via accretion, may significantly influence the venting of chemicals by clouds [*Yin et al.,* 2002, *Barth et al.*, 2007; *Cho et al.,* 1989]. Ice hydrometeors in convective clouds may form and grow due to distinct microphysical transformations. Three major categories of such transformations exist, delineated by specific environmental conditions and giving rise to distinct hydrometer types [*Pruppacher and Klett*, 1997]. These are non-rime freezing, dry-growth riming, and wet-growth riming.

Non-rime freezing involves the freezing of supercooled droplets without contact with an already frozen substrate hydrometeor. This phenomenon is normally associated with very low temperatures (< -30°C), and the associated ice nucleation may be either homogeneous or heterogeneous in nature. Hydrometeors formed via this process

generally retain the approximate shape of the original supercooled drop [*Hobbs*, 1974; *Pruppacher an Klett,* 1997].

Conversely, riming involves the collision and collection of supercooled water drops by solid substrates, which may include, ice crystals, graupel, and hail, due to the differences in velocity of the drops and substrate. Riming can be further classified into either of two broad categories: wet-growth or dry growth riming. The regime a hydrometeor grows in is greatly dependent on specific conditions of drop size, hydrometeor speed, cloud water content, and temperatures (of air, drop, and riming substrate). Wet-growth riming results in a partially frozen hydrometeor, which may contain pockets of water in the hydrometer, or on the surface of the hydrometeor, and a surface temperature of approximately 0^{o}C. Due to these conditions, drop interference and coalescence occurs, resulting in a more dense and transparent structure. Some liquid water may be shed from the riming hydrometeor. Conversely, dry-growth riming is associated with conditions of lower cloud water content and surface temperatures below 0^{o}C. Due to the low temperatures associated, drop freezing occurs independently, without coalescence, resulting in less dense, opaque hydrometeor. Because of the varying environmental conditions and processes characterizing the different freezing categories, factors affecting volatile chemicals retention in the frozen hydrometeor due to these microphysical transformations may differ significantly.

Several authors have carried out laboratory studies investigating the degree to which a volatile chemical species may be retained in the ice phase due to the riming process. Consequently, they have characterized a retention ratio, which gives the ratio of solute mass in the hydrometeor to that which was originally in the impinging droplet, i.e.,

the equilibrium concentration [Iribarne *et al.,* 1983; *Iribarne and Pyshnov*, 1990; *Lamb and Blumenstein,* 1987; *Snider and Huang*, 1998]. These investigations measured the retention efficiencies of gases found in clouds including O_2, SO_2, H_2O_2, HNO_3, HCl, and NH_3, and calculated values ranging between 0.01 and 1. Factors that varied among the studies were summarized by *Stuart and Jacobson* [2003] and included temperature, droplet and substrate size, solute concentration, pH, and impact speed.

To address the lack of understanding regarding the factors leading to the observed differences in experimentally derived retention ratios, *Stuart and Jacobson* [2003; 2004; 2006] developed theory-based retention parameterizations and a mechanistic model under conditions satisfying dry growth riming and non-rime freezing. The retention ratio was found to be highly dependent on the effective Henry's constant, drop velocity, and drop size. The formation of a complete or partial ice shell was also found to have a significant impact on retention. Chemicals with high effective Henry's constant were found to be completely retained. For those with negligible Henry's constant values, retention was found to be highly dependent on freezing conditions. However, the microphysical processes determining volatile chemical fate during ice accretion in the wet-growth regime remain poorly understood.

1.5. Thesis organization

In this study, I investigate the substrate properties, chemical characteristics, and environmental variables affecting chemical retention under conditions of wet growth. More specifically, this body of research attempts to answer the following scientific questions:

- What chemical properties affect chemical retention in hail growing under wet-growth conditions?
- What specific environmental conditions contribute to volatile chemical retention in ice hydrometeors for conditions of wet growth?
- What particle-scale microphysical process influence volatile chemical retention for accretion under wet growth conditions?

Stuart [2002] developed a mechanistic analytical equation for the evaluation of volatile chemical retention during steady-state accretion on wet growing hail. The derivation is presented again in Section 2.1, by permission of the author, for completeness. In this thesis, I develop the expressions for microphysical process variables (Section 2.2), and model parameters (Section 2.3) necessary to apply the model. Model implementation and testing are discussed in Sections 2.4 and 2.5, respectively. It is then applied (Section 3) to understand the likely dependence of partitioning on environmental conditions and hail characteristics and chemical species. Results, discussions, and conclusions are presented in Sections 4, 5, and 6, respectively.

2. Model Development

This model considers a two-phase (ice and liquid water) hail particle, growing at a steady-rate, in a region of sufficiently high cloud liquid water content to satisfy conditions for wet growth. Growth is facilitated by the collection of super-cooled water drops in the volume swept out by the falling hail particle. The fate of solutes, originally dissolved in the impinging drops, is determined by two coupled mass balances; a water mass rate balance, and a solute mass balance over the growing hail particle. Expressions describing the process governing hailstone development, such as impingement, evaporation, and shedding, are derived from cloud microphysics.

2.1 Retention ratio

Wet growth is characterized by higher surface temperatures (~0^{o}C), higher cloud water mixing ratios, and higher rates of drop impingent on the substrate, than the conditions associated with the dry-growth regime [*Pruppacher and Klett*, 1997, p. 659]. Under these conditions, impinging drops coalesce prior to freezing on the growing hailstone. This may lead to the presence of a liquid water layer (skin) on the surface of the hydrometeor and liquid water in entrapped pockets throughout the hailstone [*Johnson and Ramussen*, 1992, *Schumann*, 1938]. If the skin is thick enough, water can be shed as water droplets, due to gyration (rotation) of the hailstone [*Garcia-Garcia and List*, 1992].

Under wet-growth conditions, chemical solutes dissolved in the impacting drops may be retained in the growing hailstone, in the water film at the surface of the hail, entrapped in water pockets within hail ice, or incorporated in the ice structure. Solutes can be removed from the growing hail via shed water and through evaporation. Figure 1 illustrates the processes involved in solute retention during wet growth riming.

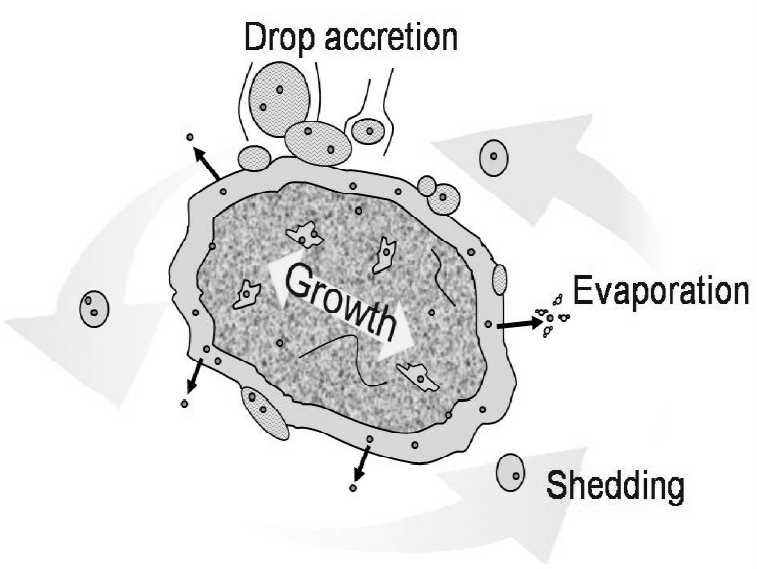

Figure 1. Hail growth and solute transfer processes.

Under constant environmental conditions (temperatures, pressure, cloud water content, and velocities), rates of water flux to the hydrometeor, water shedding, and ice growth will be approximately constant. Hence, hydrometeor growth and solute partitioning will be at a constant rate. Adapting the development of *Makkonen* [1987] for determining the salinity of sea spray ice, we can write a rate balance on solute mass during wet-growth:

$$X_d F = X_h G + X_e E + X_l S \qquad \text{Eqn (1)}$$

Here, F is the mass rate of drop collection, G is the mass rate of hydrometeor growth, E is the mass rate of solution evaporation, and S is the mass rate of shedding, each having units of mass per time. X_d, X_h, X_e, and X_l are the solute mass fractions, e.g. gram solute per gram of solution, in the drops (d), evaporated solution (e), hydrometeor (h), and surface (and shed) liquid (l). Note that this equation assumes that the liquid-to-gas mass transfer (evaporation) rate for chemical solute is proportional to that for water evaporation. This is a simplification for an open system (low concentrations of water vapor and solute in the surrounding air), similar diffusivities in air, similar Schmidt numbers, and equilibrium chemical partitioning at the liquid-gas interface.

It is noted that a water rate balance require $S = F - E - G$, and subsequent rearrangement, results in the following:

$$\frac{X_h G}{X_d F} = \frac{\left(X_h / X_l\right) G}{\left(X_h / X_l\right) G + \left(X_e / X_l\right) E + S} \qquad \text{Eqn (2)}$$

It is recognized that X_e / X_l is a mass fraction air-water distribution coefficient. In terms of the more traditional Henry's constant, it is equivalent to:

$$\frac{X_e}{X_l} = \frac{1}{H^*}\left(\frac{\rho_l}{\rho_{vl}^s}\right) \qquad \text{Eqn (3)}$$

where, H^* is the dimensionless effective Henry's constant in terms of concentration in water over concentration in air, ρ_l is the density of the liquid solution, and ρ_{vl}^s is the saturation vapor density over the liquid solution.

The term X_h/X_l can be determined using a solute mass balance on the hydrometeor given by:

$$X_h M_h = X_l M_l + X_i M_i \qquad \text{Eqn (4)}$$

$$X_h M_h = X_l M_l + X_l \left(\frac{X_i}{X_l} \right) M_i \qquad \text{Eqn (5)}$$

where, M_h, M_l, and M_i represent the total mass, liquid phase mass, and ice phase mass of the hailstone, respectively. Since, X_i is the mass fraction of solute in ice, and X_l is the mass fraction of solute in the liquid solution, X_i/X_l is an effective ice-liquid interfacial distribution coefficient, which we term k_e. It includes the effect of crystal growth rates, dendritic trapping, and convectively enhanced solute mass transfer in the liquid [*Hobbs*, 1974, p. 600 - 605]. Rearrangement of equation (4) results in:

$$\frac{X_h}{X_l} = \eta + k_e (1 - \eta) \qquad \text{Eqn (6)}$$

where, η is the mass fraction liquid water content of the hydrometeor (M_l/M_h).

To solve for the retention ratio during wet growth riming, we substitute equations (3) and (6) into equation (2) and rearrange the terms. The retention ratio or ratio of solute mass fraction in the hydrometeor to that in the original impinging drops is then given by:

$$\Gamma = \frac{G\left[\eta + k_e (1-\eta)\right]}{\underbrace{G\left[\eta + k_e (1-\eta)\right]}_{\text{Growth effect}} + \underbrace{E\left[\frac{1}{H^*}\left(\frac{\rho_l}{\rho_{vl}^s}\right)\right]}_{\text{Evaporation effect}} + \underbrace{S}_{\text{Shedding}}} \qquad \text{Eqn (7)}$$

Here, Γ represents the mass rate of chemical accumulation in the hailstone over that in the collected liquid drops, given by GX_h / FX_d , that is, the retention fraction.

2.2 Microphysical process variables

To calculate the retention ratio using Equation 7, rates of the microphysical processes involved in riming must be estimated. These include mass rates of drop collection, water evaporation, hailstone growth, and shedding.

The rate of drop collection is estimated assuming a spherical particle of radius *r*, moving with a velocity through a region of air of defined liquid water content, and sweeping out a volume determined by its cross-sectional area, πr^2. Therefore, the rate of impingement is a function of the fall speed of the hydrometeor and the liquid water content of the air. Thus, the mass rate of drop collection is given by [*Pruppacher and Klett*, 1997, p.568 – 570]

$$F = \varepsilon \pi r^2 v \omega \rho_a \qquad \text{Eqn (8)}$$

where, *v* is the fall speed of the hailstone relative to the drop, *r* is the hailstone radius, ρ_a is the density of air, ω is the mass fraction liquid water content of the cloud, and ε is the collection efficiency.

Evaporation is represented as a first-order rate process for mass transfer from liquid to air. Assuming a spherical hailstone, and an open system, the mass rate of solute evaporation, E, is then [*Pruppacher and Klett*, 1997, p. 537]:

$$E = 4\pi r D \Phi \left(\frac{P_{vl}^{s}}{R_v T_H} \right) \qquad \text{Eqn (9)}$$

where, P_{vl}^{s} is the saturation vapor pressure over liquid water, R_v is the universal gas constant for water vapor, T_H is the temperature of the hailstone, D is the diffusivity of water vapor in air, and Φ is the ventilation coefficient defining convective enhancement of evaporation due to hail motion. An open system assumption is used for consistency with the simplifying assumption of proportional rates of water and solute transfer.

The mass growth rate of the hail is the sum of the ice growth rate (G_i) and the rate of change of liquid water mass of the hydrometeor (G_w). Thus:

$$G = G_i + G_w \qquad \text{Eqn (10)}$$

where G_i is estimated [after *Stuart and Jacobson*, 2006] as:

$$G_i = 4\pi r^2 b \left(\Delta T\right)^c \rho_i \qquad \text{Eqn (11)}$$

Here, ρ_i is the density of the hailstone, and $[b(\Delta T)^c]$ is the intrinsic crystal interface growth velocity. The form of the interface growth velocity equation and factors, b and c are based on experimental data and theory for growth rates of ice in super-cooled water [*Pruppacher and Klett*, 1997, p. 668 – 674]. $\Delta T = T_0 - T_{int}$ is the super-cooled temperature of the ice liquid interface, where T_0 is the equilibrium freezing temperature of water (0˚C), and T_{int} is the ice-liquid interface temperature. As interface temperature are expected to be very close to 0°C during wet growth, we use a b of 0.3 and c of 2 for the classical growth regime [*Bolling and Tiller*, 1961].

Considering the case of constant liquid water content of the hailstone the rate of change of liquid mass of can be determined by:

$$G_w = \frac{\eta}{(1-\eta)} G_i \qquad \text{Eqn (12)}$$

The mass shedding rate of the growing hail is determined by water mass conservation as $S = F - G - E$, as defined above.

2.3 Model parameters and assumptions

Chemical and physical property and process parameters are necessary for application of the above equations. Expressions describing properties of water phase change, dry and moist air, and water vapor were defined based on available literature. Properties of the ice substrate, and super-cooled drop, such as ventilation characteristics, were similarly defined. Table 1. lists model parameters, literature references for the estimation method, and assumptions applied.

Table 1. Methods for estimation of model parameters

Parameter	Method Reference and Assumptions
Hail Temperature (T_h)	Assumed equal to 0°C
Latent heat of water melting (L_m)	*Jacobson* [2005, p. 40, Eqn. 2.55]
Latent heat of water sublimation(L_s)	*Jacobson* [2005, p. 40, Eqn. 2.56]
Latent heat of water evaporation	$L_s - L_m$; *Jacobson* [2005, p. 40, Eqn. 2.56]
Saturation vapor pressure over liquid water (P_{vl}^s)	*Jacobson* [2005, p. 41, Eqn. 2.62]
Saturation vapor density over liquid water (ρ_{vl}^s)	*Jacobson* [2005, p. 31, Eqn. 2.25]
Saturation vapor density over ice	*Jacobson* [2005, p. 43, Eqn. 2.64]
Water-air surface tension	*Jacobson* [2005, p. 485, Eqn. 14.19]
Dynamic viscosity of dry air	*Jacobson* [2005, p. 102, Eqn. 4.54]
Heat capacity of dry air at constant pressure	*Smith and Van Ness* [2001, p. 109, Table 4.1]
Partial pressure of water vapor in air (P_a)	*Jacobson* [2005, p. 21, Eqn. 2.27]
Mass mixing ratio of water vapor in air	*Jacobson* [2005, p. 32, Eqn. 2.31]
Thermal conductivity of dry air	*Jacobson* [2005, p. 20, Eqn. 2.5]
Gas constant for moist air	*Jacobson* [2005, p. 33, Eqn. 2.37]
Gas constant for water vapor (R_v)	*Jacobson* [2005, p. 22, Eqn. 2.21]
Molecular weight of moist air	*Jacobson* [2005, p. 31, Eqn. 2.26]
Density of moist air (ρ_a)	*Jacobson* [2005, p. 33, Eqn. 2.36]
Kinematic viscosity of moist air	*Jacobson* [2005, p. 102, Eqn. 4.55]
Mean free path of moist air	*Jacobson* [2005, p. 506, Eqn. 15.24]
Effective Henry Constant (H*)	*Seinfeld &Pandis* [1998, p. 340 – 350]
Heat capacity of moist air at constant pressure	*Jacobson* [2005, p. 20, Eqn. 2.5]
Diffusivity of water vapor in air (D)	*Pruppacher & Klett* [1997, p. 503, Eqn. 13-3]
Heat capacity of (supercooled) water	*Pruppacher & Klett* [1997, p. 93, Eqn. 3-16]
Density of (supercooled) liquid water (ρ_l)	*Pruppacher & Klett* [1997, p. 87, Eqn. 3-14]
Density of ice (ρ_i)	*Pruppacher & Klett* [1997, p. 9, Eqn. 3-2]
Density of hailstone (ρ_h)	$\rho_h = [(\eta/\rho_l) + ((1-\eta)/\rho_i)]^{-1}$ Weighted reciprocal average of ice and water densities.
Drop terminal fall velocity	*Jacobson* [2005, p. 664, Eqn. 20.9]
Hailstone fall velocity	*Pruppacher & Klett* [1997, p. 87, Eqn. 10-175 – 10-178], *Jacobson* [2005, p. 507, Eqn.15.26]
Impact speed of drops and hailstone (v)	Assumed equal to $v_h - v_d$.
Reynolds Number for flow around drops	*Jacobson* [2005, p. 664, Eqn. 20.6]
Reynolds Number for flow around hailstone	*Seinfeld &Pandis* [1998, p. 463, Eqn. 8.32]
Prandtl Number	*Jacobson* [2005 p. 532, Eqn. 16.32]
Schmidt Number	*Jacobson* [2005 p. 531, Eqn. 16.25]
Stokes, Nusselt, and Sherwood Numbers	*Stuart and Jacobson* [2004, Section 2.3]
Ventilation Coefficient (Φ)	*Pruppacher & Klett* [1997, p. 537, Eqn. 13-52]
Critical liquid water content (ω_c)	*Stuart and Jacobson* [2004, Eqn. 14]

Calculations of the parameters listed in Table 1. were based on several assumptions. It was assumed that the air is saturated with respect to water. Temperatures of the air, hail ice, and super-cooled drop were assumed equal, whilst, hail water temperature was assumed equal to the equilibrium freezing temperature. Saturation vapor densities and critical water limit for wet growth, as well as, the temperature dependence of the chemical specific Henry's Law constant, and dissociation constants describing pH dependence, were calculated using the equilibrium freezing temperature. Here, I used an average hail density for simplification which compared well to parameterizations developed by *Heymsfield and Pflaum* [1985] and *Macklin* [1962] for riming, based upon drop radius, a, the temperature of the ice substrate, T_s, and the impact speed of the drops, U_{imp}, (of the form, $Y = -aU_{imp}/T_s$). Drop fall velocity was calculated as discussed in *Jacobson* [2005, p. 661 - 664]. Hail fall velocity was determined accounting for the inertial effect of the particle given by the empirical drag coefficient, CD, as follows in *Seinfeld and Pandis* [1998, p. 462 - 468], with an initial hail fall speed based on parameterizations discussed in *Pruppacher and Klett* [1997, p. 441 – 444]. Symbols are provided in Table 1. for parameters used elsewhere in the text.

2.4 Implementation

Model calculations were performed using Microsoft Excel spreadsheets. Statistical ensemble modeling runs were performed using Oracle's statistical and risk analysis software, *Crystal Ball*®, to assess impact of variation in the input parameters on the modeled retention fraction. The basis of the ensemble runs is the generation of random numbers, bounded by the range previously defined for system variables of interest. That is, to assess the impact of a particular variable, it is assigned a fixed possible range, and all other system variables are assigned random values, by a random number generator, bounded by a predefined range determined by the model conditions. By choosing regular intervals within its range for the controlled variable whilst simultaneously randomly varying the values assigned to the other parameters, any statistical dependence between the manipulated variable and system parameters is established. Such probabilistic models, involving the element of chance, are called Monte Carlo simulations.

Initial simulations were performed to determine appropriate ranges for trace chemical parameters. Additional input parameters included those controlling the variability of hail and environmental factors. The range of values assigned to the input parameters were based on literature values for conditions applicable to wet growth, and each was assumed to confirm to a uniform distribution.

Chemical input variables are the effective Henry's constant and the effective ice-liquid distribution coefficient. Although the equilibrium ice-liquid distribution coefficient, k_D , is chemical specific, the effective ice-liquid distribution coefficient, k_e, is

a strong function of the kinetics of freezing and is less dependent on the specific chemical. The equilibrium ice-liquid distribution coefficient is defined as the ratio of the solute concentration directly adjacent to the interface in the solid, $C_s(i)$, to the solute concentration directly adjacent to the interface in the liquid, $C_l(i)$, as discussed by *Hobbs* [1974, p. 600]

$$k_D = \frac{C_s(i)}{C_l(i)} \qquad \text{Eqn (13)}$$

Following the discussion of *Hobbs* [1974], the equilibrium ice-liquid distribution coefficient describes the extent at which solute molecules are incorporated into the growing ice phase and is a direct measure of the distortion imposed by solute molecules on the molecular arrangement in the solid. For ionic solutes in water, k_D is always very much less than unity *Hobbs* [1974]. However, under steady-state conditions, as the solute concentration builds up in the liquid phase and diffuse away from the interface, the width of this liquid layer next to the interface may change thus affecting the localized equilibrium. Thus, it will depend on the rate of freezing, the equilibrium ice-liquid distribution coefficient, and the diffusivity of the solute molecules. Therefore, an effective ice- liquid distribution coefficient is defined by *Hobbs* [1974]:

$$k_e = \frac{C_s}{C_\infty} \qquad \text{Eqn (14)}$$

Here, C_∞ is the concentration of the bulk solution at a point far removed from the interface. Thus, k_e considers other processes affecting water-to-ice mass transfer such as

crystal growth rates, dendritic trapping, and convectively enhanced mass transfer in the liquid phase. However, based on experimental data presented by *Hobbs* [1974], and other sources cited therein, there is little variation in the derived k_e for varying chemical species, with the ranges presented having the same order of magnitude. Hence, I assume the same range of values, based on the measured effective ice-liquid distribution coefficients, for all species considered.

To determine the range of effective Henry's constants to consider, a second spreadsheet was used to calculate the pH dependent effective Henry's constant, H^*, accounting for dissociation, for each atmospherically relevant chemical species considered. Calculations were based on formulations presented in *Seinfeld and Pandis* [1998, p. 340 – 385] using tabulated values of Henry's constants, aqueous equilibrium constants, and reaction enthalpies given in Table 2. Distributions of H^* for each chemical of interest were obtained with ensemble simulations in which the pH was allowed to vary randomly with a uniform distribution from 2 to 8, and water temperature was assumed equal to the equilibrium freezing temperature. The resulting overall species maximum and minimum effective Henry's constant, derived from these simulations, was then used to define the range for subsequent calculations of retention. The results are discussed and presented in Section 4.

Table 2. Chemical properties and thermodynamic data

Chemical	[§]Henry's Law Coefficient, M/atm.	Enthalpy of Dissolution of Henry Law Coefficient, kcal/mole	1st dissociation constant, M	2nd dissociation constant, M	[†]DHC range observed
Sulfur Dioxide, SO_2	1.23	-6.25	1.3×10^{-2}	6.6×10^{-8}	6.6 – 8.5
Hydrogen Peroxide, H_2O_2	74500	-14.5	2.2×10^{-12}	-	7.2 – 8.6
Ammonia, NH_3	62	-8.17	1.7×10^{-5}	-	5.8 – 10.5
Nitric Acid, HNO_3	210000	-	15.4	-	11.2 – 18.5
Formaldehyde, CH_2O	2.5	-12.8	$2.53\times10^{+3}$	-	5.4 – 12.3
Formic Acid, HCOOH	3600	-11.4	1.8×10^{-4}	-	2.5 – 9.4

[§] Chemical properties were taken from *Seinfeld and Pandis* [1998, Chap. 6, p. 341 – 391], for values observed at 298K.

[†] DHC – dimensionless Henry's constant, was calculated at the equilibrium freezing temperature based on the temperature dependence of the Henry's constant, and other dissociation constants, given by *Seinfeld and Pandis* [1998, p. 342, Eqn. 6.5].

This model considers hail growing in the wet-growth regime. Thus, only conditions of cloud liquid water content greater than the Schumann-Ludlam limit calculated critical water content limit, W_c, for a given set of environmental conditions were considered. The Schumann-Ludlam limit, which considers a heat balance on the riming substrate, is given by [*Stuart and Jacobson,* 2004; after *Macklin & Payne,* 1967, and *Young,* 1993]:

$$W_c = \frac{f}{2\varepsilon v r\left[L_m - c_w\left(T_o - T_a\right)\right]}\left[Nuk_a\left(T_o - T_a\right) + ShDL_s\left(\rho_i^{sat} - \rho_a\right)\right] \quad \text{Eqn (15)}$$

Here, f is the shape factor of the substrate, ε is the efficiency of collection, v is the impact speed, r is the hail radius, Nu and Sh are the Nusselt and Sherwood numbers, respectively, k_a is the thermal conductivity of air, D is the diffusivity of water vapor, $c_{w,}$ is the heat capacity of water, and, L_m and L_s are the latent heats of fusion and sublimation of water vapor, respectively. Essentially, the rate per unit area at which heat is being dissipated to the environment by convection and evaporation is compared to the rate at which it is being added due to freezing of the droplets. Hence, for a given ambient temperature, air speed, and particle size, there exists a critical liquid water concentration for which all the accreted drops may be just frozen. Exceeding this critical liquid water concentration results in excess water remaining unfrozen on the hail, and growth occurs in the wet regime. For the purposes of model implementation, a wet growth boundary parameter, *WB*, was calculated for all sets of input conditions considered. If *WB* was positive ($\omega > W_c$, where ω is the cloud liquid water content as given in Table 3.), the

results were considered in our analysis. If *WB* was negative, they were only retained to understand the implications of the constraint on the overall results.

Table 3. Model input variables and ranges

Name and Symbol	Units	Range	Reference and assumptions
Hailstone diameter (D_h)	mm	1 – 50	*Pruppacher and Klett* [1997, p.71]
Hailstone liquid water content (η)	[-]	10^{-4} – 0.5	Maximum observed water fraction, *Lesins and List* [1986]
Ice interface supercooling (ΔT)	°C	10^{-4} – 10	For classical growth regime, *Pruppacher and Klett* [1997, p. 668]
Hailstone shape factor (*f*)	[-]	3.14 – 4	*Macklin and Payne* [1967], *Jayaranthe* [1993]
Collection efficiency (ε)	[-]	0.5 – 1	Assumed close to 1, *Lin et. al.* [1983]
Cloud liquid water content (ω)	gm^{-3}	2 – 5	*Pruppacher and Klett* [1997, p. 23]
Drop radius (a)	μm	5 – 100	*Jacobson,* [2005. Tab 13.1, p. 447]
Atmospheric pressure (P)	mb	200 – 1013	Tropospheric pressures, *Jacobson* [2005, App. B.1].
Air temperature (T_a)	°C	-30 – 0	Observed wet-growth regime limits, *Pruppacher and Klett* [1997, p. 682]
Effective Henry's constant (H^*)	[-]	$10^{2.5}$ – $10^{18.5}$	Calculated for pH range, *Seinfeld and Pandis* [1998, p. 340-385]
pH	-	2 – 8	Approximate range observed in experimental retention studies
Effective Ice-liquid distribution coefficient(k_e)	[-]	10^{-5} – 10^{-3}	Experimental data and theory, *Hobbs* [1974, p. 600-606]

Air temperature range was assigned based on limits to wet growth for maximum hail radius, maximum liquid water content, and minimum pressure as discussed in *Pruppacher and Klett* [1997, p. 682]. The pH occurring in the troposphere depends on the types and concentrations of dissolved chemical species present. Ranges used were based on typical midrange tropospheric pH variation as discussed in *Seinfeld and Pandis*

[1998, p. 345]. Cloud liquid water content range represents values occurring in deep convective clouds with high updrafts, as discussed in *Pruppacher and Klett* [1997, p. 23]. The range assigned to mass fraction liquid water content of the hail particle considers the higher liquid mass associated with the wet-growth regime. For higher temperatures and liquid water contents, the ice fraction assumes a constant minimum of 0.5 [*Lesins and List*, 1986]. *Pruppacher and Klett* [1997, p. 668], and other sources cited therein, discusses the dependence of ice growth rate on bath supercooling with parameterizations covering the range 0.5°C to 10°C. Here, the range assigned for ΔT accounts for lower velocities due to higher temperatures associated with the growth regime. The distribution coefficient for solute in ice is discussed in text. The collection efficiency is an assumed value, chosen between 0 and 1, but greater than 0.5 based on higher liquid water concentrations associated with the wet growth regime as discussed by *Lesins and List* [1986]. The range given for the shape factor considers that the substrate assumes geometry somewhere between a cylinder and a sphere [*Macklin and Payne*, 1967]

An additional constraint on the model was also necessary to ensure consistency between the ice growth rate and the mass available for growth. The intrinsic growth rate of the ice phase depends predominantly on the ice-liquid interface temperature, ΔT, (Equation 11) which is represented as an input variable as there is no way to determine it within the scope of this model. Consequently, some combinations of model input parameters may result in all the liquid mass on the hail freezing, thus violating the wet-growth concept. Here I defined an *allowable growth rate* by considering the amount of water mass present on the hail after accounting for evaporation $(F - E)$. A growth rate boundary parameter, *GB*, was then calculated for all sets of input conditions by

comparing the hail growth rate (see Equation 10) with the calculated allowable growth rate. If *GB* was positive, [*(F-E) >G*], the results were considered in our analysis. If *GB* was negative, they were only retained to understand the implications of the constraints on the overall results. It must be noted that the *GB* and *WB* constraints discussed above were applied simultaneously.

2.5 Testing

The validity of the data obtained from derived model parameters was assessed by comparison to published data. The temperature dependence of chemical specific Henry's constants was compared to data discussed in *Seinfeld and Pandis* [1998, p. 340 – 350] and other sources cited therein, and was found to be in good agreement. Similarly, Reynolds number averaged drop and hail settling velocities were found to compare well with data given by *Jacobson* [2005, p. 507] and, *Pruppacher & Klett* [1997].

The model was checked for conservation of water and solute mass mass balance analysis. A mass balance test on hail water mass was conducted by considering the fundamental model equation describing the water rate balance around the growing hail particle discussed in Section 2., given as, $S = F - G - E$. Since the rates of impingement, growth, and evaporation were independently derived, the mass balance consisted of equating the sum of these processes, with the mass rate of drop shedding. Perfect conservation of mass was observed for all variations of model parameters that met the model constraints.

A solute mass balance required tracking a defined mass of solute through the model logic and ensuring conservation of mass. An initial concentration of trace chemical was defined in the air phase, C_a. Its concentration in each medium was subsequently derived from the original model equations describing solute mass fraction expressions as given in Section 2.1. Thus, the mass fraction of solute in the drops, hail ice, shed liquid and evaporated solution, were calculated from the following expressions:

$$X_d = C_a\left(H^*/\rho_w\right) \qquad \text{Eqn (16)}$$

$$X_h = \Gamma X_d \qquad \text{Eqn (17)}$$

$$X_l = \frac{X_h}{\left(\eta + k_e\left(1-\eta\right)\right)} \qquad \text{Eqn (18)}$$

$$X_e = X_l\left(\frac{1}{H^*}\right)\left(\frac{\rho_l}{\rho_{vl}^s}\right) \qquad \text{Eqn (19)}$$

Multiplying these solute mass fraction expressions with the appropriate water mass rates gives the solute mass accumulation rate in each compartment. Perfect conservation of solute mass was observed for all variations of model parameters that meet the model constraints.

3. Application

To investigate the dependence of retention on environmental, microphysical, and chemical factors, retention ratios were calculated for a range of chemicals of atmospheric interest using an ensemble modeling approach. Six trace chemicals were considered, namely, SO_2, H_2O_2, NH_3, HNO_3, CH_2O, and HCOOH. Appropriate ranges for H^* were first calculated for these species as discussed in Section 2.4 using a 100 member ensemble.

With the Effective Henry's Constant range defined, a modified Monte Carlo ensemble modeling approach was then used to determine the dependence of retention on input variables. In this approach, a series of ensemble simulations was run for each input variable previously defined. The focus variable of each series was held constant at discrete values uniformly spaced over the range listed in Table 3. For each of those values, a 100-member ensemble was assembled by allowing all other variables to vary randomly over a continuous uniform distribution defined by the range of each variable as listed in Table 3. Only those results meeting the model constraints were retained in the analysis. Resulting output distributions of retention ratios and constraint conditions are presented and discussed in Section 4.

4. Results

The results generated from modified Monte Carlo ensemble runs were categorized and presented by type as, hail factors (mass fraction liquid water content of hail, η, hail diameter, D_h, hail shape factor, f, ice-liquid interface temperature, ΔT, and hail collection efficiency, ε), chemical factors (effective Henry's constant, H^*, and effective ice-liquid distribution coefficient, k_e), and environmental factors (air temperature, T_a, pressure, P, cloud liquid water content, ω, and drop radius, a).

4.1 Hail factors

4.1.1. Hail diameter

Result of the dependence of simulated retention on hail diameter is shown in Figure 2(a). The mean simulated retention varied between 0.068 and 0.15 for distinct hail diameters, with an overall distribution range of 5.1×10^{-6} to 0.88. No clear trend is observed between the mean or other distribution parameters of the retention ratio and hail diameter. Although no clear dependence of retention on hail diameter can be ascertained, a trend was observed in the number of ensemble members within model constraints (see bold numbers in Figure 2a). The number of valid runs was observed to increase with increases in diameter.

From Equation 8, an increase in hail diameter is expected to result in an increase the drop collection rate, F, by increasing the swept volume of drops collected. Hail fall

velocity (and hence impact velocity) also increases with hail diameter, also increasing *F*. From Equation 9, it is expected that increasing hail diameter will result in an increase the evaporation rate, *E*, through increased surface area and ventilation, *f*. Since the particle Reynolds number is proportional to its radius and fall speed, greater ventilation is expected with increases in diameter, which further enhances vapor and energy transfer processes. The hail diameter also affects the critical liquid water content, which indirectly affects retention. Finally, hail diameter has effects on shedding due to effects on hail motion, but this is not captured in this model. Here, shedding, *S*, will increase if *F* increases or *E* or *G* (mass growth rate) decrease. Hence, overall a complicated relationship between hail diameter and retention is expected, due to the counteracting effects of *F*, *S*, and *G* on retention (see Equation 7). The lack of observed dependence on hail diameter indicates that no one effect dominates. Additionally, the large range indicates that other parameters or combinations of parameters are more important to controlling retention.

Results of the dependence of the constraint parameters on hail diameter are shown in Figure 3(a) and 4(a). It was observed that as hail diameter increases, the mean of the growth rate boundary parameter, *GB*, increases slightly (i.e. becomes more positive), with fewer member runs outside the boundary (less negative values). However, larger variability in *GB* is observed as the hail diameter increases, indicating that as hail diameter increases, the influence of other input parameters of the growth rate of the hail becomes more pronounced. As previously mentioned, hail diameter is expected to have a direct correlation with drop collection rate and water evaporation rate. For the wet growth boundary parameter, *WB*, shown by Figure 4(a), a trend of increasing mean *WB*

parameter with increasing hail diameter is observed. Equation 15 indicates that as hail diameter increases the calculated critical water content for wet growth will decrease, thus increasing the *WB* parameter. As hail diameter increases, an increase in the number of valid simulation runs is also observed, as well as, a decrease in the variability of the *WB* parameter. This indicates that as hail diameter increases, the influence of the other input parameters on the growth regime decreases.

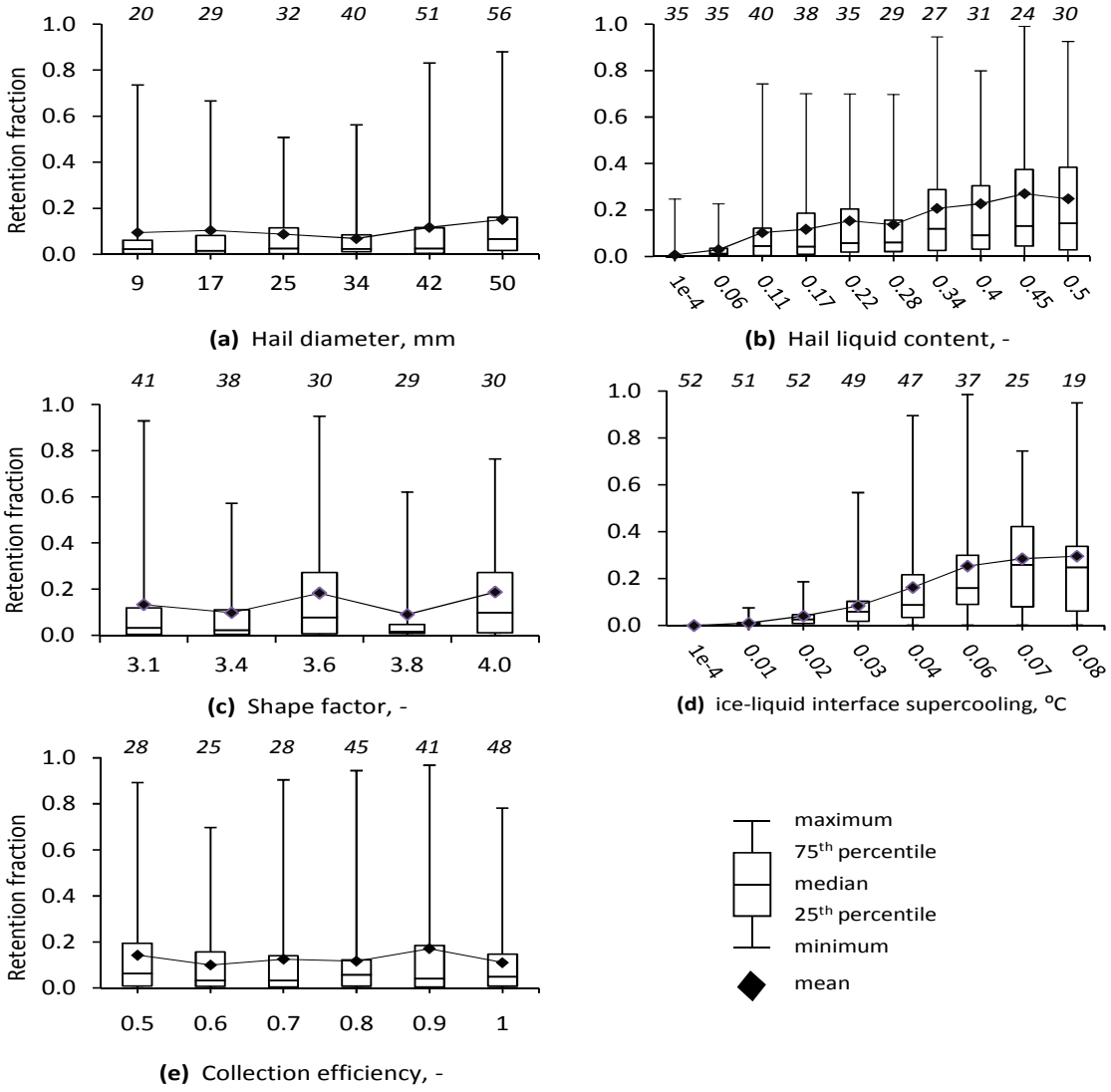

Figure 2. The effect of individual hail input variables on retention fraction. The box plots characterize the ensemble distribution of simulated results with the abscissa held constant and other parameters varied randomly. The italicized value above each box plot provides the number of ensemble member runs that met model constraints.

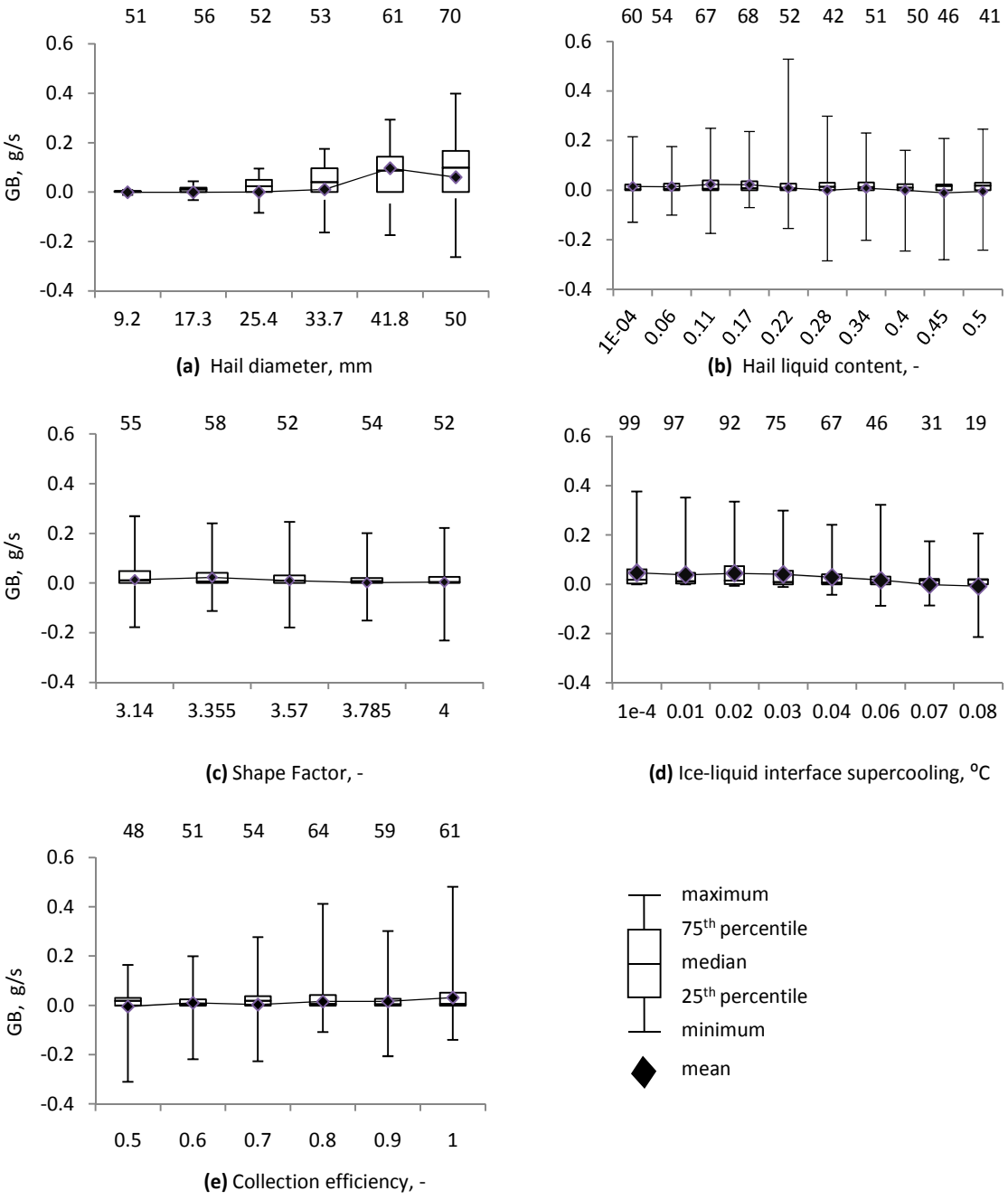

Figure 3. The effect of individual hail input variables on the growth rate boundary parameter, GB. The box plots characterize the ensemble distribution of simulated results with the abscissa held constant and other parameters varied randomly. The italicized value above each box plot provides the number of ensemble member runs that met model constraints.

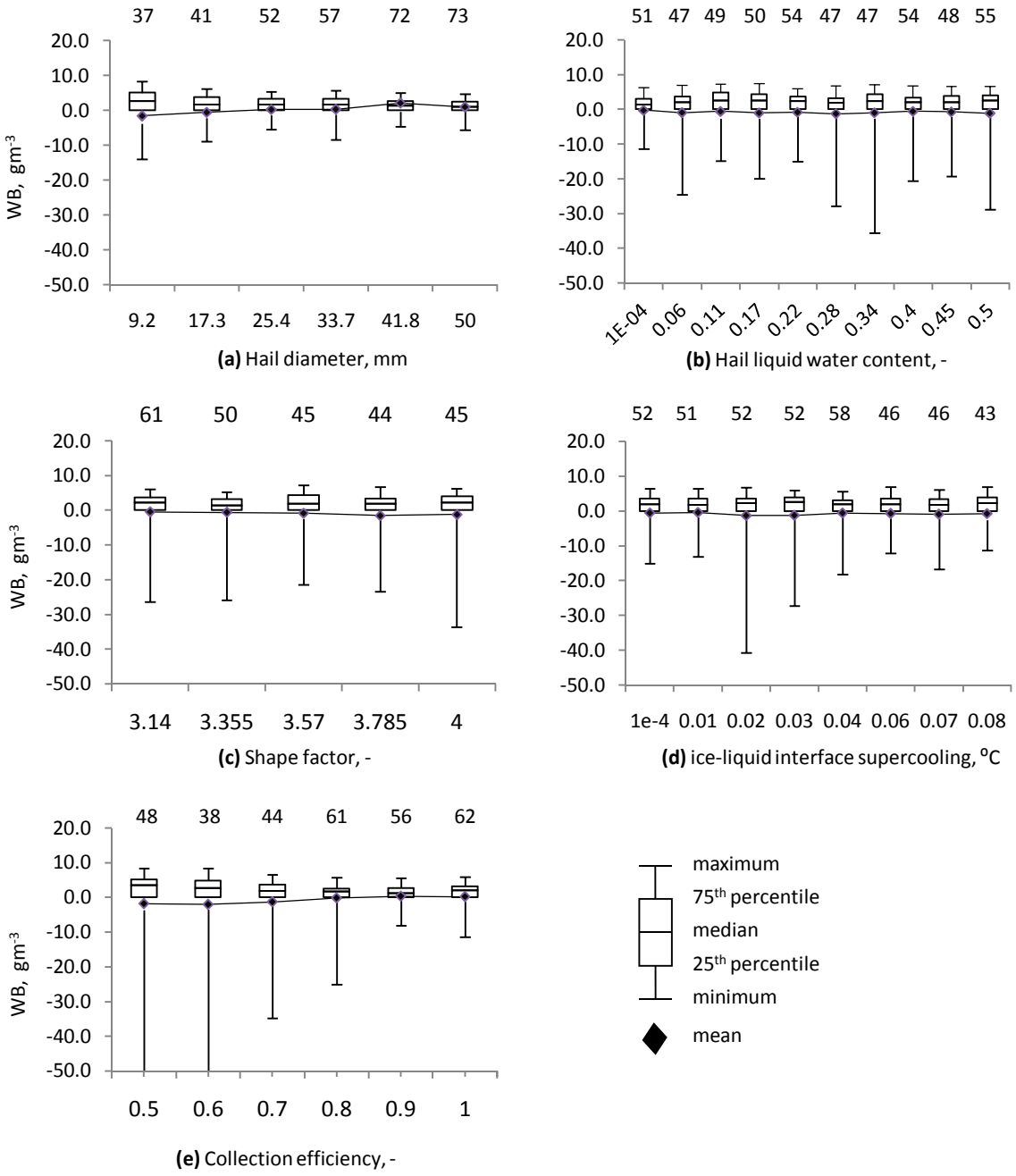

Figure 4. The effect of individual hail input variables on the wet growth boundary parameter, WB. The box plots characterize the ensemble distribution of simulated results with the abscissa held constant and other parameters varied randomly. The italicized value above each box plot provides the number of ensemble member runs that met model constraints.

4.1.2. Mass fraction liquid water content of hail

The effect of hail liquid water content, η, on retention is shown in Figure 2(b). Mean simulated retention varied from 7.5×10^{-3} to 0.27 with increasing η, exhibiting a strong dependence of retention on the mass fraction liquid water content of the hail. The overall range observed ranged from 6.0×10^{-8} to 0.99, with no obvious trend in variability, or number of valid runs with changes in η.

From Equation 7, a direct dependence of the retention ratio on η is observed in the numerator. This is because as η increases, with comparatively negligible partitioning to ice (significantly low k_e), more solute can be stored in the liquid (X_l) (see Equation 6). However, the retention ratio is also indirectly influenced by η through its effects on hail growth, *G,* and shedding, *S*. It is expected that increasing η will result in an increase in the growth rate of the hail as indicated by Equations10 and 12. Shedding is determined by conservation of water mass, so as growth rate increases, shedding decreases (with *E* constant) with the resultant opposite effect on the retention ratio. Since an increasing trend of retention with increases in η is observed, it can be surmised that the direct (numerator) effect and/or shedding dominate the growth effect.

The effect of η on the constraint parameters is shown in Figure 3(b) and 4(b). No definite trend is observed between the mean and values of *GB* or *WB* and hail water fraction. As η increases, an increase in the variability of the *GB* parameter was observed, indicating increasing influence of other input parameters on the growth rate. Additionally, for *WB*, extremely high negative values were observed for some

combination of the input parameters, suggesting that there were combinations of input parameters that strongly affect the growth regime.

4.1.3. Ice-liquid interface temperature

Figure 2(d) gives the results of simulated retention on the ice-liquid interface temperature, ΔT. Mean simulated retention increased fom 9.0×10^{-7} to 0.30 with increasing ΔT, indicating a dependence of retention on ΔT. The overall range varied between 1.1×10^{-4} and 0.99 with increasing variability as ΔT increased. The number of valid runs converely decreased with increasing ΔT (closer to zero) .

From Equation 11, it is expected that as ΔT increases, the intrinsic growth rate of the hail ice will increase, thus increasing the overall hail growth rate, G. From Equation 7, is is expected that the quantity termed the *growth effect* will increase with increasing G, leading to a subsequent decrease in retention. However, this is countered by the indirect effect of shedding. Here, an increase in G leads to a decrease in the shedding term, which has a greater influence, and results in an general increase in the observed retention.

The effect of ΔT on the growth rate boundary prameters is shown in Figures 3(d) and 4(d). There is no significant dependence observed between the mean or other distribution parameter of the GB parameter and ΔT. However, a definite decrease in the number of valid model runs is observed as ΔT increases via its direct effect on the intrinsic ice growth rate, subsequently affecting the model constraint directly. For WB

no definite trend exists in the mean values, but there is an observed decrease in the variability of *WB* as ΔT increased.

4.1.4. Hail shape factor

The dependence of simulated retention ratio on the shape factor, *f*, is shown in Figure 2(c). The mean retention varies from 0.91 to 0.19, with an overall distribution range of 1.3×10^{-6} to 0.95. There is no definite relationship observed between the mean or other distribution parameter of the modeled retention ratio and shape factor.

Since the shape factor only appears in the wet growth boundary constraint, Equation 15, it can only influence retention through that constraint. From Equation 15, it is observed that the shape factor influences the heat balance on the riming substrate by determinig the enhancement of energy transfer due to the curvature of the interface [*Macklin*, 1964]

Figure 3(c) gives the effect of the hail shape factor on the growth rate boundary constraint. There is no relationship observed between the distribution parameters of the growth rate boundary and the the shape factor. A direct relationship between the shape factor and the growth boundary is not expected. However, large variations in the distribution of the *GB* parameter is observed, due to combination of effects of the other input parameters.

The effects of the shape factor on the wet growth boundary parameter is given by Figure 4(c). The was no trend observed between the shape factor and the distribution parameters describing the wet growth boundary. From Equation 15 it is expected that as the particle transitions from a cylinder to a sphere, the critical liquid water required for it

to remain in the wet growth regime will increase, thus influencing the *GB*. However, it is also affected by the ambient temperature, particle size, and the impact speed. Thus, no direct correlation is observed. High variability in the *GB* simulations is observed with higher negative values. There was no variation in the number of valid model runs, however.

4.1.5. Efficiency of collection

Figure 2(e) characterizes the effect of the collection efficiency, ε, of the hail on the simulated retention ratio. Mean retention ranged from 0.10 to 0.17, and the overall distribution indicated possible values ranging from 2.8×10^{-6} to 0.97. No clear trend is observed in the mean or variability of the simulated retention ratio.

From Equation 8 it is expected that, as ε increases, the mass rate of drop collection increases. As given by Equation 7, the effect of an increase in drop collection depends on the relative rates of shedding, evaporation and ice growth. Since no trend is observed, no one effect appears to dominate.

The influence of the collection efficiency on the growth rate boundary is shown by Figure 3(e). There is no trend observed between the distribution parameters of the simulated growth rate boundary parameter and the collection efficiency. Also , no trend is observed in the variability of the *GB* parameter with changes in collection effeciency, although high overall vairability in the data. This indicates that there is no direct effect of the collection efficiency on the constraint.

Figure 4(e) gives the relationship between the collection efficiency and the wet growth boundary parameter. There is no definite trend observed between the collection

efficiency and the distribution parameters characterizing the growth regime boundary. Additionally, there is no trend observed in the variability of the *GB* parameter distribution. However, greater negative values is observed in the distribution. The collection effeciency is not expected to significantly impact the growth regime of the particle.

4.2 Environmental factors

4.2.1. Cloud liquid water content

The dependence of the simulated retention ratio on the cloud liquid water content, ω, is shown in Figure 5(a). The mean of the simulated retention ratio varied between 0.11 and 0.21. The overall distribution ranges from 1.1×10^{-6} to 0.96. There is no relationship observed between ω and the distribution parameters describing the modeled retention ratio.

The direct effect of an increase in the cloud liquid water content is an increase in the rate of drop collection on the hail, as given by Equation 8. Following Equation 7, this should result in a decrease in the growth and evaporation effect, and a corresponding increase in retention. However, due to the counteracting effects of drop shedding, a definite trend is not observed.

The dependence of the growth rate boundary on cloud liquid water content is given by Figure 6(a). There is a perceptible trend observed between the mean of the *GB* parameter and ω, with the *GB* increasing with increases in ω. However, there is no trend observed in the variability of *GB* or the number of valid model runs.

Figure 7(a) shows the relationship between the cloud liquid water content and the wet growth boundary parameter. The mean of the *WB* parameter is observed to increase slightly with increasing cloud liquid water. It is expected that parameter to increase with increasing cloud liquid water, since it is defined by comparing the calculated critical liquid water content of the hail to the actual cloud liquid water content. However, I do acknowledge that other parameters, such as the particle size, ambient temperature, and impact speed play important role in the calculated critical water content. The distribution of the *GB* parameter showed no obvious trend in variation, but was negatively skewed. It is observed that as the cloud liquid water increases, the number of valid model runs increases. This is expected, since as mention previously, the boundary is based on the comparison of the calculated critical liquid water content with the observed cloud liquid water.

4.2.2. Drop radius

The dependence of the simulated retention ratio on drop radius is shown by Figure 5(b). The mean of the simulated retention ratio is observed to vary from 0.12 to 0.15. The overall range of variability of retention ratio was between 4.9×10^{-5} and 1.1. There was no significant trend observed in mean or variability of the simulated retention ratio with changes in drop radius.

It is expected that as drop radius increases, it may lead to a decrease in the impact speed, due to the decrease in relative velocities of drop and hail particle, and a subsequent decrease in the drop collection term in Equation 8. The effect of a decrease in drop

collection depends on the relative rates of the other model parameters, *E*, *S,* and *G*, as discussed previously.

The effect of drop radius on the growth rate boundary parameter is characterized by Figure 6(b). No trend is observed between the mean or other distribution parameter of the *GB* parameter and the drop radius. Based on the definition of the growth rate boundary, there is no indication of a direct relationship between the drop radius and the growth boundary parameter. Similarly, though there was some amount of variability in the *GB* parameter, no trend was observed in the variability. Additionally, no trend was observed between drop radius and the number of model runs meeting the model constraint.

Figure 7(b) gives the relationship between the wet growth boundary parameter and the drop radius. There is no trend observed between the mean or other distribution parameter of the WB parameter and the drop radius. From Equation 13, the drop radius is expected to impact the critical liquid water content required for wet growth by affecting the rate of heat dissipation of the freezing drop. This may result in greater water mass on the hail and consequently a decrease in the critical water content required. However, no trend was observed indicating a relationship between drop radius and growth regime observed. Additionally, no trend was observed in the number of valid model runs.

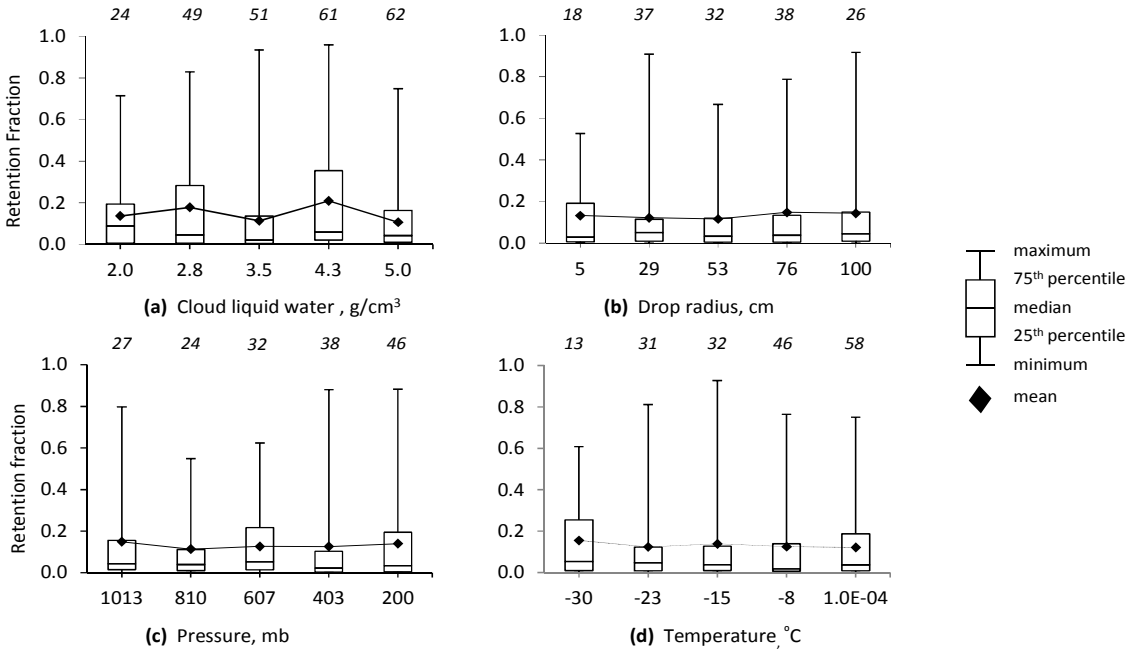

Figure 5. The effect of individual environmental input variables on the retention fraction. The box plots characterize the ensemble distribution of simulated results with the abscissa held constant and other parameters varied randomly. The italicized value above each box plot provides the number of ensemble member runs that met model constraints.

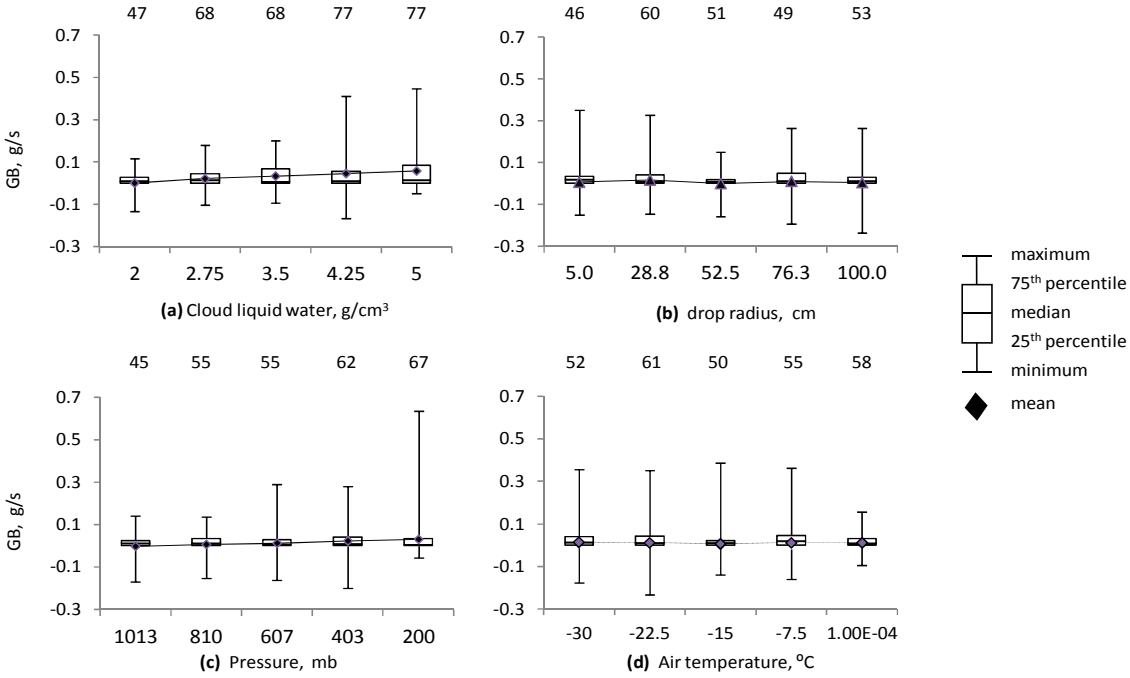

Figure 6. The effect of individual environmental input variables on the growth rate boundary parameter, GB. The box plots characterize the ensemble distribution of simulated results with the abscissa held constant and other parameters varied randomly. The italicized value above each box plot provides the number of ensemble member runs that met model constraints.

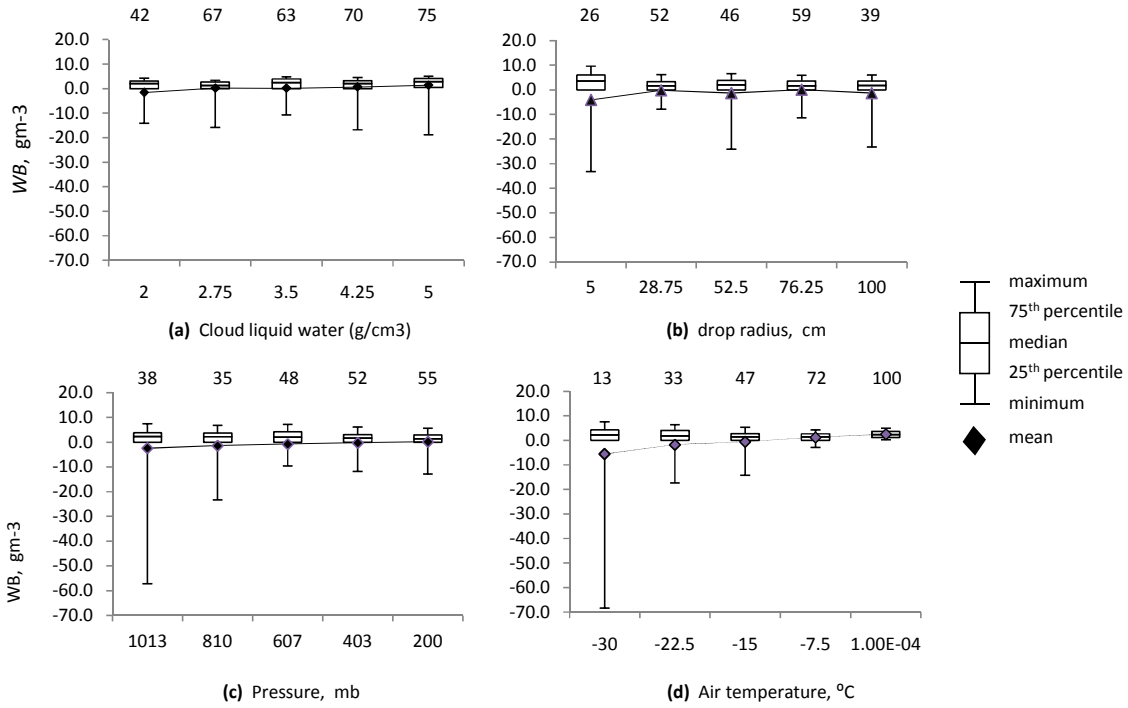

Figure 7. The effect of individual environmental input variables on the wet growth boundary parameter, WB. The box plots characterize the ensemble distribution of simulated results with the abscissa held constant and other parameters varied randomly. The italicized value above each box plot provides the number of ensemble member runs that met model constraints.

4.2.3. Pressure

Figure 5(c) characterizes the effect of pressure on the modeled retention ratio. The mean simulated retention ratio varied from 0.11 to 0.15, whilst the overall distribution had a minimum value of 1.3×10^{-8} and a maximum value 0.88. There was no clear relationship observed between the mean retention and pressure, though the variability appears to decrease as pressure increases. The number of valid model runs increased gradually, as the pressure increased.

As pressure decreases, an increase in the diffusivity of water vapor is expected, leading to a subsequent increase in solution evaporation as given by Equation 9, and a

decrease in retention. However, it, may also directly lead to a decrease in the shedding term and subsequently an increase in the modeled retention ratio. No one effect appears to dominate.

The effect of pressure on the growth rate parameter is shown by Figure6(c). There is no trend observed between the distribution parameters describing the growth rate parameter and pressure. Greater variability, as well as, an increase in the number of valid model runs was observed.

Figure 7(c) characterizes the effect of pressure on the wet growth parameter. There is no clear trend observed between the mean or other distribution parameter defining the wet growth boundary and pressure. The variability of the *WB* parameter appears negatively skewed, with extremely large negative values, but there appears to be no clear trend in the variability. However, the number of valid model runs showed an increase as pressure decreased.

4.2.4. Air temperature

The dependence of the simulated retention ratio on the temperature of air is shown in Figure 5(d). Whilst the mean retention ratio varied between 0.12 and 0.16, the overall range observed varied from 5.6×10^{-6} to 0.93. There was no apparent individual effect on the mean retention fraction due to variation in air temperature. An increase in the number of valid model runs with increasing temperature is observed,

Some anticipated direct effects of temperature on the retention ratio include its effect on solution evaporation, by affecting both the diffusivity and the solution saturated vapor density. From Equation 9, it is expected that that these two terms would generate

opposite effects on solute evaporation. Hence, the relationship between retention and temperature is expected to be complex.

Figure 6(d) shows the relationship between temperature and the growth rate boundary. There is no trend observed between the growth rate boundary distribution parameters and temperature. Based on the definition of the *GB* parameter, it is expected that, as temperature increases, it may increase the mass rate of solution evaporation, thus leading to a decrease in the growth boundary. Additionally, no trends in the variability of the distribution of the *GB* parameter with increases in temperature are observed. There is also no observed effect of temperature on the number of valid model runs.

Figure 7(d) characterizes the relationship between the wet growth boundary parameter and temperature. There is a relationship observed between the growth boundary parameter and temperature, with the *WB* parameter increasing as temperature increases. From Equation 13, a complex relationship between temperature and the wet growth boundary parameter is expected. A definite increase in the number of valid model simulations is observed as temperature increased, as well as a decrease in the variability of the WB parameter distribution indicating a relationship between the model constraint and temperature.

4.3 Chemical factors

4.3.1. Chemical effective Henry's constant and pH

Figure 8(a) characterizes the dependence of the simulated retention ratio on the effective Henry's constant, H^*. The mean retention varied between 1.6×10^{-3} and 0.17, whilst the distribution parameters show retention varying between 1.4×10^{-4} and 0.79. A trend is observed between H^* and the mean of the simulated retention ratio. An increase in retention is observed as the Henry's constant increases. There is no observed trend in the variation of valid model simulations with changes in the effective Henry's constant. Additionally, no trend in the variation of the retention ratio distribution is observed, as H^* is increased.

From Equation 7, it is expected that as the effective Henry's constant increases, the evaporation term decreases, that is, the evaporate-to-liquid solution chemical mass rate ratio decreases, thus resulting in an increase in retention. However, it is also recognized that drop shedding, which also depends on the solute evaporation term, plays a large role in determining the retention fraction, where, as the evaporation term decreases, it leads to an increase in the shedding term, and a subsequent reduction in retention would result. As an increasing trend is observed, it is expected that the direct effect of evaporation dominate that of shedding. It must be noted that the effective Henry's constant is significantly dependent on pH. The range used for effective Henry's constant model simulations were derived based on the dependence of the effective Henry's constant on pH as shown by Figure 8(c). As the figure shows, the effective Henry's constant for acidic species (HNO_3, SO_2) increases by orders of magnitude as pH

increases from 4 to 7, whilst, the opposite effect is seen for basic species (NH_3). Hence, since retention is affected by H^*, it is also significantly affected by pH.

Figure 9(a) shows the effect of the effective Henry's constant on the growth boundary parameter. There is no trend observed by the distribution parameters characterizing the model constraints and H^*. Additionally, no trend was observed in the variation of the growth boundary. There was no effect of H^* on the number of valid model runs observed.

The effect of the effective Henry's constant on the wet growth boundary parameter is shown by Figure 10(a). There is no trend observed in the mean of the wet growth boundary or any of the other distribution parameters describing the GB parameter with variations of H^*. Large negative values were observed in the minimum distribution parameter but there was no definite trend in the variation observed.

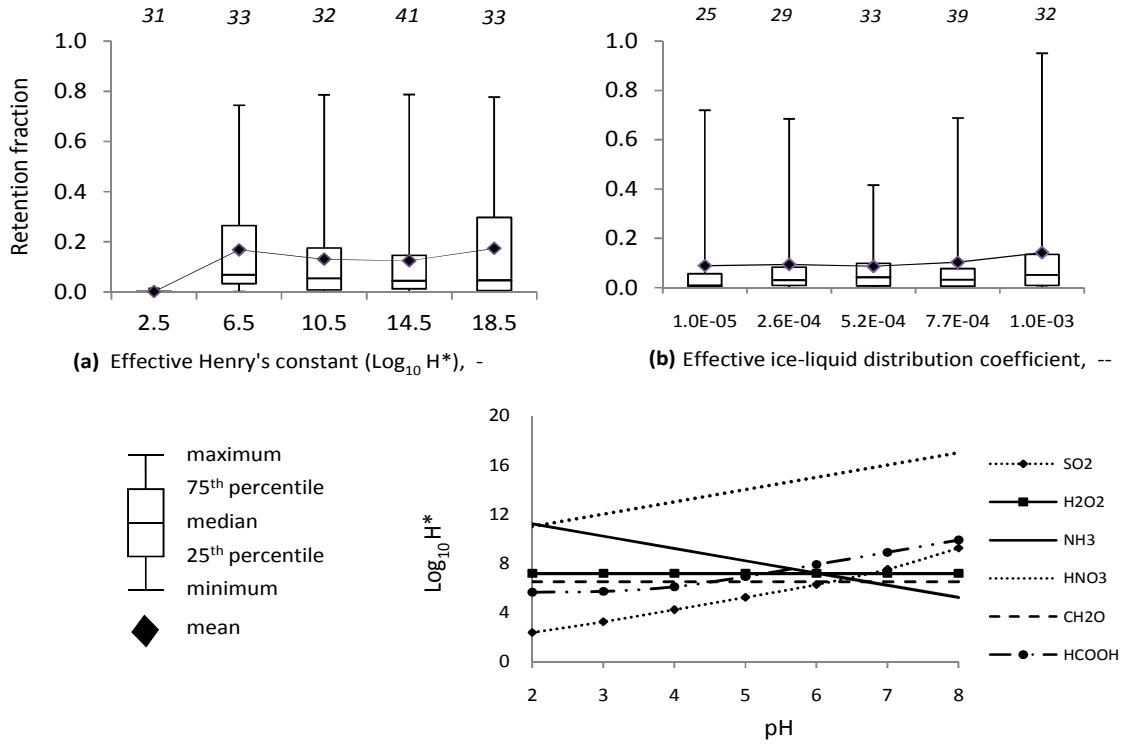

Figure 8. The effect of individual chemical input variables on the retention fraction. The box plots characterize the ensemble distribution of simulated results with the abscissa held constant and other parameters varied randomly. The italicized value above each box plot provides the number of ensemble member runs that met model constraints.

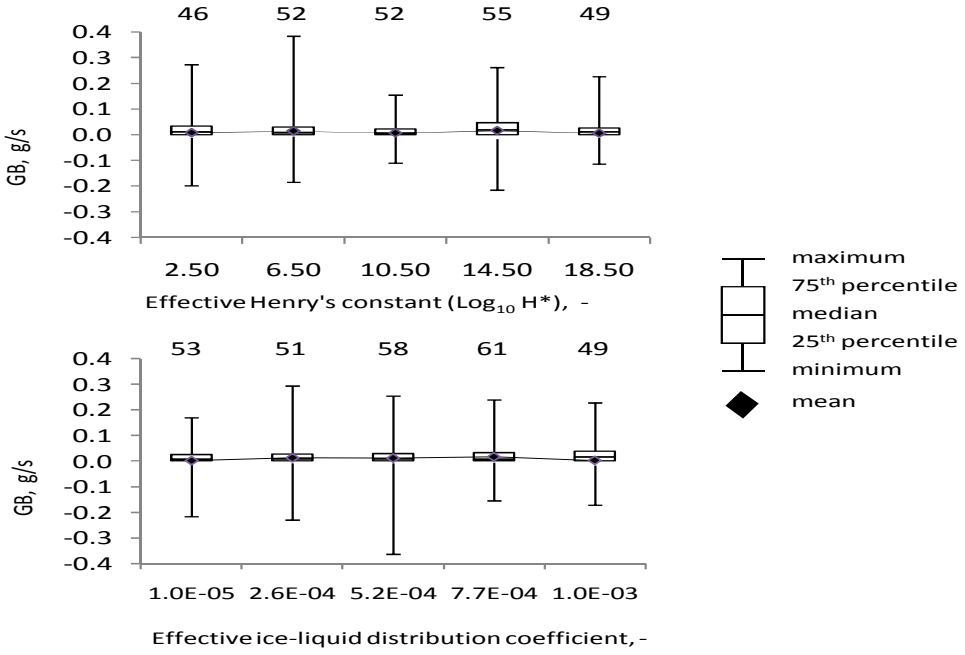

Figure 9. The effect of individual chemical input variables on the growth rate boundary parameter, GB. The box plots characterize the ensemble distribution of simulated results with the abscissa held constant and other parameters varied randomly. The italicized value above each box plot provides the number of ensemble member runs that met model constraints.

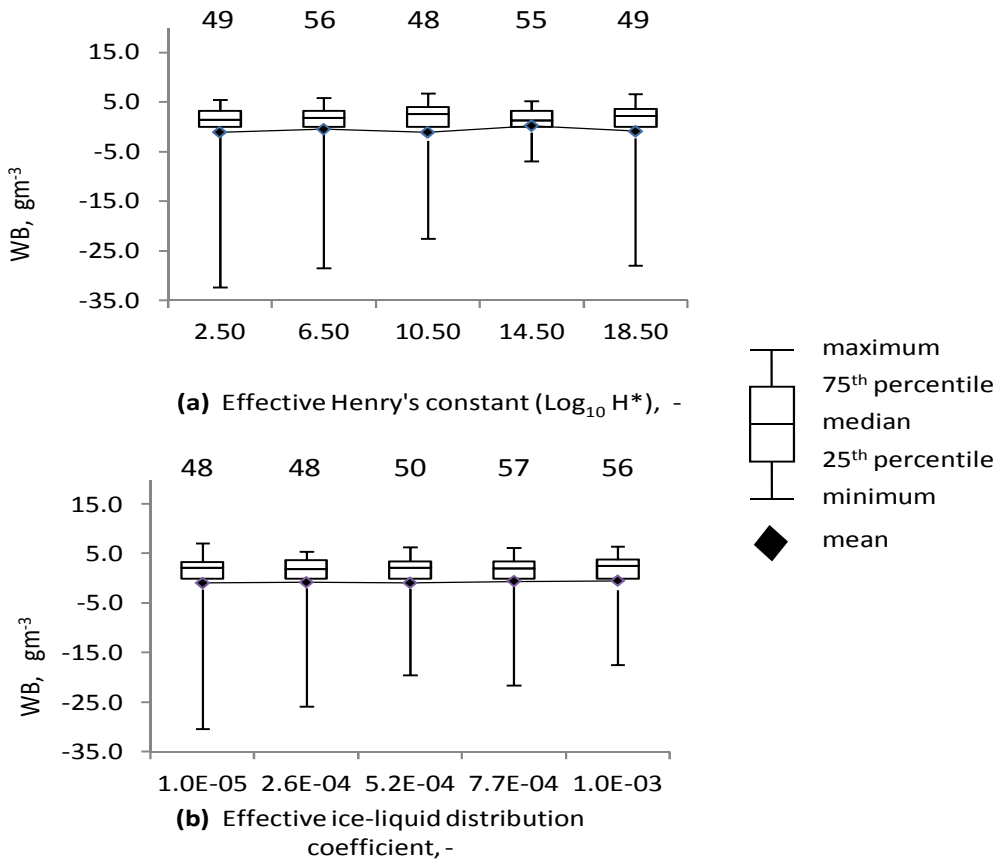

Figure 10. The effect of individual chemical input variables on the wet growth boundary parameter, WB. The box plots characterize the ensemble distribution of simulated results with the abscissa held constant and other parameters varied randomly. The italicized value above each box plot provides the number of ensemble member runs that met model constraints.

4.3.2. The effective ice-liquid distribution coefficient

The effect of the effective ice-liquid distribution on the simulated retention ratio is shown in Figure 9(b). The mean simulated retention varied between 0.087 and 0.14, whilst the minimum and maximum distribution parameters varied between 5.2×10^{-6} and 0.95. There is no trend observed between the mean or other distribution parameters characterizing the simulated retention ratio and the effective ice-liquid distribution coefficient.

From Equation 7 it is expected that as k_e increases, both the numerator and denominator will increase. However, due to the magnitude of k_e, ($\sim 10^{-4}$), it has little influence.

The effect of k_e on the model constraints is characterized by Figure 10(b).There was no trend observed by the distribution parameters characterizing the model constraints and k_e. There was no trend observed between the number of valid model parameters observed and variation in effective ice-liquid distribution coefficient.

The effect of the ice-liquid distribution coefficient on the wet growth boundary parameter is given by Figure 11(b). There was no trend observed in the mean of the WB parameter and k_e. Similarly, no trend was observed in the variability in the distribution parameters, however, greater negative (minimum) values were observed.

4.4 Summary of results

Table 3 provides a summary of the parameters investigated and their observed effect on the retention ratio as given by the simulations conducted. The ice- liquid interface temperature, ΔT, hail liquid water fraction, and the chemical's effective Henry' constant, were found to individually affect retention, with retention increasing as each of the parameters were increased. The cloud liquid water content, ω, and collection efficiency, ε, showed possible inverse relationship with the retention ratio. All the other parameters do not alone appear to have a clear relationship with the retention ratio. Maximum values of retention observed were clearly not resulting from any particular model parameter, but rather from a combination of model parameters. Finally, retention ratios greater than 1.0 were observed for certain combinations of conditions.

Table 4. Dependence of simulated retention fraction on input variables

Parameter	Effect Description	Range of Ensemble Means	Overall Range
Interface supercooling, ΔT	Large, direct, monotonic	9.0×10^{-8} – 0.30	1.1×10^{-8} – 0.99
Mass fraction hail liquid water content, η	Large, direct	7.5×10^{-3} – 0.27	6.0×10^{-8} – 0.99
Chemical's effective Henry's constant, H^*	Large, direct, levels off	1.6×10^{-3} – 0.17	1.4×10^{-4} – 0.79
Cloud liquid water content, ω	Very small, non-monotonic	0.11 – 0.21	1.1×10^{-6} – 0.96
Hail shape factor, f	Very small, non-monotonic	0.091 – 0.19	1.3×10^{-6} – 0.95
Hail diameter, D_h	Very small, non-monotonic	0.068 – 0.15	5.1×10^{-6} – 0.88
Collection efficiency, ε	Very small, non-monotonic	0.10 – 0.17	2.8×10^{-6} – 0.97
Effective ice-liquid distribution coefficient, k_e	None	0.087 – 0.14	6.2×10^{-6} – 0.95
Air temperature, T_a	None	0.12 – 0.16	5.6×10^{-6} – 0.93
Atmospheric pressure, P	None	0.11 – 0.15	1.3×10^{-8} – 0.88
Drop radius, a	none	0.12 – 0.15	4.9×10^{-5} – 0.92

5. Discussion and Limitations

The model presented explores the partitioning of volatile chemical species during rime freezing under wet growth conditions. In an attempt to understand and predict the retention of atmospherically relevant gases, I investigated the environmental factors, and hail and chemical properties influencing this process.

The ice-liquid interface supercooling was found to be the most important forcing variable for solute retention during wet growth of hail. Experimental studies have found a direct relationship between retention and supercooling under mixed wet and dry growth conditions [*Lamb and Blumenstein*, 1987; *Iribarne et al*, 1990; *Snider et al.*, 1992]. In this study, retention was found to increase as supercooling increased (lower interface temperatures) The ice-liquid interface temperature determines the intrinsic growth rate of the hail ice, but more importantly, it is influenced by the generated heat of freezing released by impinging drops, and its dissipation. This model assumes that the hailstone is growing in a cloud containing super-cooled water droplets with temperature equal to that of air. Since both the freezing of deposited water droplets and the condensation of water molecules are always accompanied by the release of latent heat, it is evident that through the period of growth, the temperature of the hail will be greater than that of the surrounding atmosphere [*List,* 1963(a); 1963(b)]. At steady-state growth, the temperature of the interface is such that the rate of heat liberation due to the deposition and freezing of water equals the rate of heat dissipation from the ice-liquid interface. Therefore,

processes that facilitate the removal or transfer of the heat of freezing released, contribute to the increased growth of the hail. These include the movement of the hail particle through the air, which increases ventilation processes and the increase in the available surface area for heat transfer, as well as, lower ambient temperatures. For the growth rate of ice in supercooled water, we used the parameterizations of *Bolling and Tiller* [1961] for the intrinsic crystal growth rate. Since the growth rate of ice is heat dissipation limited, an energy balance on the growing hail would be a better representation of the hail growth process.

Results from our model simulation find that retention of volatile solutes in hail was also significantly impacted by the mass fraction hail liquid water content of the growing hail particle. For conditions of high hail liquid mass fraction, high retention ratios were generally predicted by the model. Therefore, conditions contributing to higher hail liquid mass fraction may result in higher degrees of retention being observed. With higher liquid water content, more solute can be retained in the liquid water portion of the hail. Additionally, an overall hail particle can often contain layers formed during alternating wet and dry growth [*Pruppacher and Klett*, 1997, p. 73]. Since much of the solute is retained in the liquid during wet growth, it is expected that rate of formation of a surface ice layer during the transition to dry growth will be important to final retention. For dry growth conditions, a surface layer of ice was found to be important to trapping solute at higher concentration than would be expected from ice-air equilibrium solute partitioning [*Stuart and Jacobson*, 2003, 2004, 2006]. However, in this model, the hail liquid mass fraction is explicitly set. In reality, it should be dependent on conditions such as temperature, impingement rates, and shedding rates. Shedding has been determined by

a mass balance on the water mass on the hail. However, this parameter has proven to be very influential in the determination of the effect of many other model parameters on the fraction retained. Thus, to elucidate the direct and indirect effects of parameters such as the hail mass fraction, and hail diameter on retention, an explicit representation of this process is required in future work, where drop shedding is a function of drop impingement, hail motion, and properties of the water phase.

Chemical Henry's constant was found to be the third important determinant of retention fractions, with higher fractions observed for higher effective Henry's constants (more soluble, less volatile chemicals). This is consistent with previous findings for dry growth conditions and experiment studies discussed therein [*Stuart and Jacobson*, 2003, 2004]. However, under wet growth conditions, the chemical Henry's constant (and pH) are likely less important than for dry growth conditions, with only a low mean value of retention (0.2) simulated for the highest considered effective Henry's constant. Hence, under wet growth conditions, the chemical identity is not expected to be as important to determining partitioning as for dry growth. The range generated for use in the modified Monte Carlo simulations was based on observed variation of H* with changes in pH (over the range 4 – 7).

There was no direct relationship observed between the effective ice-liquid distribution coefficient and the retention ratio. Distribution coefficients for chemical species in ice occur over the range 10^{-3} – 10^{-5} [*Hobbs*, 1974]. Subsequently, model simulations indicate the effects of the ice-liquid distribution coefficient may not be influential to solute retention. This may be considered advantageous since the effective ice-liquid distribution coefficient is poorly characterized.

Overall, the issue of co-dependence and indirect effects on retention through independently varied hail parameters decreases our confidence in findings for the environmental variables (cloud liquid water content, air temperature, atmospheric pressure, and drop radius). The environmental variables may affect the hail liquid water content and/or the interface supercooling temperature, which were found to significantly force retention. Hence, to better understand the impacts of environmental variables, it will be important to calculate these two hail variables within the model, rather than set them independently as input variables. This will require calculation of the shedding rate independent of the water mass balance and a heat balance calculations. For the other hail-related parameters (collection efficiency, hail shape factor, and hail diameter) and for the effective ice-liquid chemical distribution coefficient, no clear effect was observed on retention. Hence, it is less important to represent their dependence on environmental conditions or consider their effects on retention. As collection efficiency, hail shape factor, and the ice-liquid distribution coefficient are poorly understood themselves and would be difficult to calculate from physical (non-empirical) principles, this result is helpful to future micro- and cloud-scale modeling. Also, the very small impact of hail diameter on retention is important to the applicability of this model. Since hail diameter has no effect on retention, the assumption of a constant value is appropriate. Other model variables have no discernable effect alone on the retention fraction. These include hail diameter and cloud liquid water content. However, since many of these parameters will determine the hail liquid mass fraction, and the effective ice-liquid distribution parameters, in reality the full influence of these parameters on the fraction retained is not captured by the model.

Finally, despite high predicted maximum values for all ensemble simulations (of 0.9 - 1), the means for all ensembles were much lower, with the highest mean predicted at 0.3. Hence, no single variable was found to be responsible for simulated maximum values of retention. Rather, combinations of favorable input conditions were needed to generate retention fractions greater than 0.3. Further investigation of variable combinations that lead to the high observed values is needed.

6. Conclusions and Implications

This investigation developed and explored the process of wet growth riming, and its effect on the retention of trace atmospheric gases in growing hailstones. From cloud microphysics literature, expressions representing the important process occurring at the particle scale, such as solution evaporation and drop collection, were developed. Model parameters and calculated variables were checked and found to be consistent with previously established experimental and theoretical values. The model was checked for conservation of water and solute mass, and was consistent for all conditions satisfying model constraints.

Results generated from model simulations indicate that the most important forcing variable for solute retention during wet growth is the ice-liquid interface supercooling. The modeled retention faction for wet growing hail was also found to be largely dependent on the mass fraction of liquid water present on the hail particle. The chemical's Henry's constant was found to have significant impacts on retention, largely influencing the mass of chemical in the evaporated solution. Results also indicate that the effective ice-liquid distribution coefficient does not significantly affect retention. Shedding was observed to be an important process affecting the retention ratio and needs to be explicitly represented in future work. Direct effects of hail and drop sizes on the retention ratio were not observed.

This body of work provides a valuable insight into the hail properties, chemical properties, and environmental conditions important to predicting the fate of volatile trace gases, of atmospheric interest, due to their interaction with the growing ice phase. It is hoped that the insights gained can be used to develop better parameterizations of retention for cloud modeling studies.

7. List of References

Andrady A. et al. (2008), Environmental effects of ozone depletion and its interactions with climate change: Progress report, 2007, *Photochemical & Photobiological Sciences*, 7(1), 15-27.

Atlas D. and F. H. Ludlam (1961), Multi-wavelength radar reflectivity of hailstorms, *Quarterly Journal of the Royal Meteorological Society,* 87(374), 523-534.

Audiffren N., M. Renard, E. Buisson, and N. Chaumerliac (1998), Deviations from the Henry's law equilibrium during cloud events: A numerical approach of the mass transfer between phases and its specific numerical effects, *Atmospheric Research,* 49(2), 139-161.

Audiffren N., S. Cautenet, and N. Chaumerliac (1999), A modeling study of the influence of ice scavenging on the chemical composition of liquid-phase precipitation of a cumulonimbus cloud, *Journal of Applied Meteorology*, 38(8), 1148-1160.

Avila E. E., N. E. Castellano, and C. P. R. Saunders (1999), Effects of cloud-droplet spectra on the average surface-temperature of ice accreted on fixed cylindrical collectors, *Quarterly Journal of the Royal Meteorological Society*, 125(555), 1059-1074.

Avila E. E., R. G. Pereyra, N. E. Castellano, and C. P. R. Saunders (2001), Ventilation coefficients for cylindrical collectors growing by riming as a function of the cloud droplet spectra, *Atmospheric Research,* 57(2), 139-150.

Bailey I. H. and W. C. Macklin (1968), The surface configuration and internal structure of artificial hailstones, *Quarterly Journal of the Royal Meteorological Society,* 94(399), 1-11.

Bailey I. H. and W. C. Macklin (1968), Heat transfer from artificial hailstones, *Quarterly Journal of the Royal Meteorological Society*, 94(399), 93-98.

Baker R. A. (1967), Trace organic contaminant concentration by freezing--I. Low inorganic aqueous solutions, *Water Research*, 1(1), 61-64.

Baker R. A. (1967), Trace organic contaminant concentration by freezing--II: Inorganic aqueous solutions, *Water Research*, 1(2), 97-113.

Baker R. A. (1969), Trace organic contaminant concentration by freezing--III. Ice washing, *Water Research*, 3(9), 717-730.

Barth M. C., P. J. Rasch, J. T. Kiehl, C. M. Benkovitz, and S. E. Schwartz (2000), Sulfur chemistry in the National Center for Atmospheric Research Community Climate Model: Description, evaluation, features, and sensitivity to aqueous chemistry, *Journal of Geophysical Research,* 105(D1), 1387 - 1415.

Barth M. C., A. L. Stuart, and W. C. Skamarock (2001), Numerical simulations of the July 10, 1996, stratospheric-tropospheric experiment: Radiation, aerosols, and ozone (Sterao)-deep convection experiment storm: Redistribution of soluble tracers, *Journal of Geophysical Research*, 106(D12), 12,381–312,400.

Barth M. C., P. G. Hess, and S. Madronich (2002), Effect of marine boundary layer clouds on tropospheric chemistry as analyzed in a regional chemistry transport model, *Journal of Geophysical Research*, 107(D11), 4126.

Barth M. C., S. W. Kim, W. C. Skamarock, A. L. Stuart, K. E. Pickering, and L. E. Ott (2007), Simulations of the redistribution of formaldehyde, formic acid, and peroxides in the 10 July 1996 stratospheric-tropospheric experiment: Radiation, aerosols, and ozone deep convection storm, *Journal of Geophysical Research-Atmospheres*, 112(D13), 24.

Bertram A. K., T. Koop, L. T. Molina, and M. J. Molina (2000), Ice formation in $(NH_4)_2SO_4$-H_2O particles, *Journal of Physical Chemistry Atmospheres*, 104(3), 584-588.

Bertram T. H.et al (2007), Direct measurements of the convective recycling of the upper troposphere, *Science*, 315(5813), 816-820.

Blackmore R. Z., and E. P. Lozowski (1998), A theoretical spongy spray icing model with surficial structure, *Atmospheric Research*, 49(4), 267-288.

Bolling G. F. and W. A. Tiller (1961), Growth from the melt III. Dendritic growth, *Journal of Applied Physics*, 32(12), 2587-2605.

Browning K. A., F. H. Ludlam, and W. C. Macklin (1963), The density and structure of hailstones, *Quarterly Journal of the Royal Meteorological Society*, 89(379), 75-84.

Browning K. A. (1966), The lobe structure of giant hailstones, *Quarterly Journal of the Royal Meteorological Society*, 92(391), 1-14.

Brunner D., J. Staehelin, and D. Jeker (1998), Large-scale nitrogen oxide plumes in the tropopause region and implications for ozone, *Science*, 282(5392), 1305-1309.

Burton J. A., R. C. Prim, and W. P. Slichter (1953), The distribution of solute in crystals grown from the melt. Part I. Theoretical, *Journal of Chemical Physics*, 21(11), 1987-1991.

Carras J. N. and W. C. Macklin (1975), Air bubbles in accreted ice, *Quarterly Journal of the Royal Meteorological Society*, 101(427), 127-146.

Carstens J. C., A. Williams, and J. T. Zung (1970), Theory of droplet growth in clouds: II. Diffusional interaction between two growing droplets, *Journal of Atmospheric Sciences*, 27(5), 798-803.

Carte A. E. (1966), Features of transvaal hailstorms, *Quarterly Journal of the Royal Meteorological Society*, 92(392), 290-296.

Castellano N. E., O. B. Nasello, and L. Levi (2002), Study of hail density parametrizations, *Quarterly Journal of the Royal Meteorological Societ,* 128(583), 1445-1460.

Chameides W. L. (1984), The photochemistry of a remote marine stratiform cloud, *Journal of Geophysical Research*, 89(D3), 4739–4755.

Chang J. S., R A Brost, I S A Isaksen, S Madronich, P Middleton, W R Stockwell, C J Walcek (1987), A three-dimensional eulerian acid deposition model: Physical concepts and formulation, *Journal of Geophysical Research*, 92(14), 14,681–614,700.

Chatfield R. B., and P. J. Crutzen (1984), Sulfur dioxide in remote oceanic air: Cloud transport of reactive precursors, *Journal of Geophysical Research*, 89(D5), 7111 - 7132.

Chen J.-P., and D. Lamb (1994), The theoretical basis for the parameterization of ice crystal habits: Growth by vapor deposition, *Journal of the Atmospheric Sciences*, 51(9), 1206-1222.

Chen J.-P. and D. Lamb (1999), Simulation of cloud microphysical and chemical processes using a multicomponent framework. Part II: Microphysical evolution of a wintertime orographic cloud, *Journal of the Atmospheric Sciences*, 56(14), 2293-2312.

Cheng L., and D. C. Rogers (1988), Hailfalls and hailstorm feeder clouds - an Alberta case study, *Journal of Atmospheric Sciences*, 45(23), 3533-3545.

Cho H. R., M. Niewiadomski, J. V. Iribarne, and O. Melo (1989), A model of the effect of cumulus clouds on the redistribution and transformation of pollutants, *Journal of Geophysical Research,* 94(D10), 12895-12910.

Cober S. G., and R. List (1993), Measurements of the heat and mass transfer parameters characterizing conical graupel growth, *Journal of Atmospheric Sciences*, 50(11), 1591-1609.

Cosby B. J., G. M. Hornberger, and J. N. Galloway (1985), Modeling the effects of acid deposition: Assessment of a lumped parameter model of soil water and streamwater chemistry, *Water Resources Research*, 21(1), 51- 63.

Cosby B. J., G. M. Hornberger, and J. N. Galloway (1985), Modeling the effects of acid deposition: Assessment of a lumped parameter model of soil water and streamwater chemistry, *Water Resources Research*, 21(1), 51-63.

Daum P. H., S. E. Schwartz, and L. Newman (1984), Acidic and related constituents in liquid water stratiform clouds, *Journal of Geophysical Research*, 89(D1), 1447-1458.

David G. (2001), Estimation of entrainment rate in simple models of convective clouds, *Quarterly Journal of the Royal Meteorological Society,* 127(571), 53-72.

Dickerson R. R.et al (1987), Thunderstorms: An important mechanism in the transport of air pollutants, *Science*, 235(4787), 460-465

Dockery D. W., J. Cunningham, A. I. Damokosh, L. M. Neas, J. D. Spengler, P. Koutrakis, J. H. Ware, M. Raizenne, and F. E. Speizer (1996), Health effects of acid aerosols on North American children: Respiratory symptoms, *Environmental Health Perspectives*, 104(5), 500-505.

Domine F. and P. B. Shepson (2002), Air-snow interactions and atmospheric chemistry, *Science*, 297(5586), 1506-1510.

Federer B. and A. Waldvogel (1978), Time-resolved hailstone analyses and radar structure of Swiss storms, *Quarterly Journal of the Royal Meteorological Society*, 104(439), 69-90.

Flossmann A. I., W. D. Hall, and H. R. Pruppacher (1985), A theoretical study of the wet removal of atmospheric pollutants. Part I: The redistribution of aerosol particles captured through nucleation and impaction scavenging by growing cloud drops, *Journal of Atmospheric Science*, 42(6), 583-606.

Flossmann A. I., H. R. Pruppacher, and J. H. Topalian (1987), A theoretical study of the wet removal of atmospheric pollutants. Part II: The uptake and redistribution of $(NH_4)_2SO_4$ particles and SO_2 gas simultaneously scavenged by growing cloud drops, *Journal of Atmospheric Science,* 44(20), 2912-2923.

Ford A. (1999), *Modeling the environment: An introduction to system dynamics models of environmental systems*, Island Press, Washington, D.C.

García-García F. and R. List (1992), Laboratory measurements and parameterizations of supercooled water skin temperatures and bulk properties of gyrating hailstones, *Journal of the Atmospheric Sciences*, 49(22), 2058-2073.

Gaviola E. and F. A. Fuertes (1947), Hail formation, vertical currents, and icing of aircraft, *Journal of the Atmospheric Sciences,* 4(4), 116-120.

Giaiotti D. B. and F. Stel (2006), The effects of environmental water vapor on hailstone size distributions, *Atmospheric Research*, 82(1-2), 455-462.

Gimson N. R. (1997), Pollution transport by convective clouds in a mesocale model, *Quarterly Journal of the Royal Meteorological Society*, 123(543), 1805-1828.

Griggs D. J., and T. W. Choularton (1986), A laboratory study of secondary ice particle production by the fragmentation of rime and vapor-grown ice crystals, *Quarterly Journal of the Royal Meteorological Society*, 112 (471), 149-163.

Hegg D. A., P. V. Hobbs, and L. F. Radke (1984), Measurements of the scavenging of sulfate and nitrate in clouds, *Atmospheric Environment (1967)*, 18(9), 1939-1946.

Heymsfield A. J. (1982), A comparative study of the rates of development of potential graupel and hail embryos in high plains storms, *Journal of the Atmospheric Sciences*, 39(12), 2867-2897.

Heymsfield A. J. and J. C. Pflaum (1985), A quantitative assessment of the accuracy of techniques for calculating graupel growth, *Journal of the Atmospheric Sciences*, 42(21), 2264-2274.

Hobbs P. V. (1974), *Ice physics*, 1st. ed., Oxford University Press, Oxford.

Iribarne J. V., L. A. Barrie, and A. Iribarne (1983), Effect of freezing on sulfur dioxide dissolved in supercooled droplets, *Atmospheric Environment (1967)*, 17(5), 1047-1050.

Iribarne J. V. and T. Pyshnov (1990), The effect of freezing on the composition of supercooled droplets--I. Retention of HCl, HNO_3, NH_3 and H_2O_2, *Atmospheric Environment. Part A. General Topics*, 24(2), 383-387.

Iribarne J. V., T. Pyshnov, and B. Naik (1990), The effect of freezing on the composition of supercooled droplets--II. Retention of S(iv), *Atmospheric Environment. Part A. General Topics*, 24(2), 389-398.

Iribarne J. V. and L. A. Barrie (1995), The oxidation of S(iv) during riming by cloud droplets, *Journal of Atmospheric Chemistry,* 21(2), 97-114.

Jacobson M. Z. (2005), *Fundamentals of atmospheric modeling*, 2nd ed., Cambridge University Press, New York.

Jaeglé L., D. J. Jacob, W. H. Brune, and P. O. Wennberg (2001), Chemistry of hox radicals in the upper troposphere, *Atmospheric Environment*, 35(3), 469-489.

Jameson A. R. and A. B. Kostinski (2000), The effect of stochastic cloud structure on the icing process, *Journal of the Atmospheric Science,* 57(17), 2883-2891.

Johnson D. B. and R. M. Rasmussen (1992), Hail growth hysteresis, *Journal of Atmospheric Sciences,* 49(24), 2525-2532.

Jouzel J., L. Merlivat, and B. Federer (1985), Isotopic study of hail: The δd-δ18o relationship and the growth history of large hailstones, *Quarterly Journal of the Royal Meteorological Society*, 111(468), 495-516.

Kelly T. J., P. H. Daum, and S. E. Schwartz (1985), Measurements of peroxides in cloudwater and rain, *Journal of Geophysical Research*, D5(90), 7861–7871.

Khvorostyanov V. I. and J. A. Curry (1999), Toward the theory of stochastic condensation in clouds. Part i: A general kinetic equation, *Journal of the Atmospheric Sciences,* 56(23), 3985-3996.

Knight N. C. (1983), Measurement and interpretation of hailstone density and terminal velocity, *Journal of the Atmospheric Sciences*, 40(6), 1510-1516.

KrÄMer M., C. Schiller, H. Ziereis, J. Ovarlez, and H. Bunz (2006), Nitric acid partitioning in cirrus clouds: The role of aerosol particles and relative humidity, *Tellus B*, 58(2), 141-147.

Lamb D. and R. Blumenstein (1987), Measurement of the entrapment of sulfur dioxide by rime ice, *Atmospheric Environment (1967)*, 21(8), 1765-1772.

Latham J. and C. P. R. Saunders (1970), Experimental measurements of the collection efficiencies of ice crystals in electric fields, *Quarterly Journal of the Royal Meteorological Society*, 96(408), 257-265.

Lelieveld J. and P. J. Crutzen (1991), The role of clouds in tropospheric photochemistry, *Journal of Atmospheric Chemistry*, 1991(3), 229-267.

Lelieveld J. and P. J. Crutzen (1994), Role of deep cloud convection in the ozone budget of the troposphere, *Science*, 264(5166), 1759-1761.

Lesins G. B. and R. List (1986), Sponginess and drop shedding of gyrating hailstones in a pressure-controlled icing wind tunnel, *Journal Of Atmospheric Sciences*, 43(23), 2813-2825.

Levi L. and M. E. Saluzzi (1996), Effects of ice formation on convective cloud development, *Journal of Applied Meteorology*, 35(9), 1587-1595.

Levi L. and L. Lubart (1998), Modelled spongy growth and shedding process for spheroidal hailstones, *Atmospheric Research*, 47-48, 59-68.

Levi L., N. E. Castellano, O. B. Nasello, and F. Prodi (1999), Requirements for low density riming and two-stage growth on atmospheric particles, *Atmospheric Research*, 50(1), 21-35.

Likens G. E., C. T. Driscoll, and D. C. Buso (1996), Long-term effects of acid rain: Response and recovery of a forest ecosystem, *Science*, 272(5259), 244-246.

Lin Y.-L., R. D. Farley, and H. D. Orville (1983), Bulk parameterization of the snow field in a cloud model, *Journal of Applied Meteorology*, 22(6), 1065-1092.

List R. (1959a), Wachstum von eis-wassergemischen im hagelversuchskanal*, Helvetica Physica Acta,* 32, 293-296.

List R. (1963), General heat and mass exchange of spherical hailstones, *Journal of Atmospheric Sciences*, 20(3), 189-197.

List R. (1963), The accretion of ice on rotating cylinders, *Quarterly Journal of the Royal Meteorological Society*, 89(382), 551-555.

List R. (1966), A hail tunnel with pressure control, *Journal of the Atmospheric Sciences*, 23(1), 61-66.

List R., and J.-G. Dussault (1967), Quasi steady state icing and melting conditions and heat and mass transfer of spherical and spheroidal hailstones, *Journal of the Atmospheric Sciences*, 24(5), 522-529.

List R., J.-G. Cantin, and M. G. Ferland (1970), Structural properties of two hailstone samples, *Journal of the Atmospheric Sciences*, 27(7), 1080-1090.

Lozowski E. P. and R. Amours (1980), A time-dependent numerical model for spherically symmetric hailstone growth thermodynamics under constant ambient conditions, *Journal of the Atmospheric Sciences*, 37(8), 1808-1820.

Ludlam F. H. (1950), The composition of coagulation-elements in cumulonimbus, *Quarterly Journal of the Royal Meteorological Society*, 76(327), 52-58.

Macklin W. C. and F. H. Ludlam (1961), The fall speeds of hailstones, *Quarterly Journal of the Royal Meteorological Society*, 87(371), 72-81.

Macklin W. C., B. F. Ryan (1962), On the formation of spongy ice, *Quarterly Journal of the Royal Meteorological Society*, 88(378), 548-549.

Macklin W. C. (1962), The density and structure of ice formed by accretion, *Quarterly Journal of the Royal Meteorological Society*, 88(375), 30-50.

Macklin W. C. (1962), Accretion in mixed clouds the density and structure of ice formed by accretion, *Quarterly Journal of the Royal Meteorological Society*, 88(377), 342-343.

Macklin W. C. (1963), Heat transfer from hailstones, *Quarterly Journal of the Royal Meteorological Society*, 89(381), 360-369.

Macklin W. C. (1964), Factors affecting the heat transfer from hailstones, *Quarterly Journal of the Royal Meteorological Society,* 90(383), 84-90.

Macklin W. C., and I. H. Bailey (1966), On the critical liquid water concentrations of large hailstones, *Quarterly Journal of the Royal Meteorological Society*, 92(392), 297-300.

Macklin W. C., and G. S. Payne (1967), A theoretical study of the ice accretion process, *Quarterly Journal of the Royal Meteorological Society,* 93(396), 195-213.

Macklin W. C. and I. H. Bailey (1968), The collection efficiencies of hailstones, *Quarterly Journal of the Royal Meteorological Society*, 94(401), 393-396.

Macklin W. C., L. Merlivat, and C. M. Stevenson (1970), The analysis of a hailstone, *Quarterly Journal of the Royal Meteorological Society*, 96(409), 472-486.

Macklin W. C., J. N. Carras, and P. J. Rye (1976), The interpretation of the crystalline and air bubble structures of hailstones, *Quarterly Journal of the Royal Meteorological Society*, 102(431), 25-44.

Matson R. J. and A. W. Huggins (1980), The direct measurement of the sizes, shapes and kinematics of falling hailstones, *Journal Of Atmospheric Sciences*, 37(5), 1107-1125.

Matson R. J. and A. W. Huggins (1980), The direct measurement of the sizes, shapes and kinematics of falling hailstones, *Journal of the Atmospheric Sciences*, 37(5), 1107-1125.

Molders N., H. Hass, H. J. Jakobs, M. Laube, and A. Ebel (1994), Some effects of different cloud parameterizations in a mesoscale model and a chemistry transport model, *Journal of Applied Meteorology*, 33(4), 527-545.

Noone K. J., J. A. Ogren, K. B. Noone, A. Hallberg, S. Fuzzi, and J. A. Lind (1991), Measurements of the partitioning of hydrogen peroxide in a stratiform cloud*, *Tellus*, 43(3), 280-290.

Orville H. D.,and F. J. Kopp (1977), Numerical simulation of the life history of a hailstorm, *Journal of the Atmospheric Sciences*, 34(10), 596-1618.

Orville a. D., P. A. Eckhoff, J. E. Peak, J. H. Hirsch, and F. J. Kopp (1981), Numerical simulation of the effects of cooling tower complexes on clouds and severe storms, *Atmospheric Environment (1967)*, 15(5), 823-883.

Park R. J., K. E. Pickering, D. J. Allen, G. L. Stenchikov, and M. S. Fox-Rabinovitz (2004), Global simulation of tropospheric ozone using the University of Maryland Chemical Transport Model (UMD-CTM): 2. Regional transport and chemistry over the central United States using a stretched grid, *Journal of Geophysical Research,* 109(D09303).

Pflaum J. C., J. J. Martin, and H. R. Pruppacher (1978), A wind tunnel investigation of the hydrodynamic behaviour of growing, freely falling graupel, *Quarterly Journal of the Royal Meteorological Society*, 104(439), 179-187.

Pickering K. E., A. M. Thompson, J. R. Scala, W.-K. Tao, R. R. Dickerson, and J. Simpson (1992), Free tropospheric ozone production following entrainment of urban plumes into deep convection, *Journal of Geophysical Research*, 97(D16), 17,985-918,000.

Pitter R. L. and H. R. Pruppacher (1973), A wind tunnel investigation of freezing of small water drops falling at terminal velocity in air, *Quarterly Journal of the Royal Meteorological Society*, 99(421), 540-550.

Prather M. J. and D. J. Jacob (1997), A persistent imbalance in HO_x and NO_x photochemistry of the upper troposphere driven by deep tropical convection, *Geophysical Research Letters*, 24(24), 3189–3192.

Prodi F. (1970), Measurements of local density in artificial and natural hailstones, *Journal of Applied Meteorology*, 9(6), 903-910.

Prodi F., C. T. Nagamoto, and J. Rosinski (1980), A preliminary study of ice grown by droplet accretion using water-insoluble particles as tracer, *Journal of Applied Meterology*, 19(3), 284-289.

Prodi F., G. Santachiara, and A. Franzini (1986), Properties of ice accreted in 2-stage growth, *Quarterly Journal of the Royal Meteorological Society*, 112(474), 1057-1080.

Pruppacher H. R. and J. D. Klett (1997), *Microphysics of clouds and precipitation*, 2nd ed., Kluwer Academic Publishers, MA.

Rasmussen R. M. and A. J. Heymsfield (1987), Melting and shedding of graupel and hail. Part I: Model physics, *Journal of Atmospheric Sciences*, 44(19), 2754-2763.

Ridley B.et al (2004), Convective transport of reactive constituents to the tropical and mid-latitude tropopause region: I. Observations, *Atmospheric Environment*, 38(9), 1259-1274.

Ridley B.et al (2004), Convective transport of reactive constituents to the tropical and mid-latitude tropopause region: I. Observations, *Atmospheric Environment*, 38(9), 1259-1274.

Roos D. v. D. S., H. Schooling, J. C. Vogel, and D. O. Triegaardt (1977), Deuterium in hailstones collected on 29 november 1972, *Quarterly Journal of the Royal Meteorological Society*, 103(438), 751-767.

Rutledge S. A., D. A. Hegg, and P.V.Hobbs (1986), A numerical model for sulfur and nitrogen scavenging in narrow cold-frontal rainbands 1. Model description and dicussion of microphysical fields, *Journal of Geophysical Research*, 91(D13), 14385 - 14402.

Salzmann M., M. G. Lawrence, V. T. J. Phillips, and L. J. Donner (2007), Model sensitivity studies regarding the role of the retention coefficient for the scavenging and redistribution of highly soluble trace gases by deep convective cloud systems, *Atmospheric Chemistry and Physics*, 7(8), 2027-2045.

Santachiara G., F. Prodi, and F. Vivarelli (1995), Scavenging of SO_2 and HCl during growth of ice crystals by vapor diffusion, *Atmospheric Environment*, 29(9), 983-987.

Schumann T. E. W. (1938), The theory of hailstone formation, *Quarterly Journal of the Royal Meteorological Society,* 64(273), 3-21.

Seinfeld J. H. and S. N. Pandis (1998), Atmospheric *chemistry and physics: From pollution to climate change*, John Wiley and Sons, New York.

Snider J. R., and J. Huang (1998), Factors influencing the retention of hydrogen peroxide and molecular oxygen in rime ice, *Journal of Geophysical Research*, 103(D1), 1405 - 1416.

Solomon K. R., X. Tang, S. R. Wilson, P. Zanis, and A. F. Bais (2003), Changes in tropospheric composition and air quality due to stratospheric ozone depletion, *Photochemical & Photobiological Sciences*, 2(1), 62-67.

Stevens B., W. R. Cotton, and G. Feingold (1998), A critique of one- and two-dimensional models of boundary layer clouds with a binned representations of drop microphysics, *Atmospheric Research*, 47-48, 529-553.

Stockwell W. R., P. Middleton, J. S. Chang, and X. Tang (1990), The second generation regional acid deposition model chemical mechanism for regional air quality modeling, *Journal of Geophysical Research*, 95(D10), 16,343 -316,367.

Stuart A. L. (2002), Volatile chemical patitioning during cloud hydrometeor freezing and its effects on tropospheric chemical distributions, Ph.D. thesis, 295 pp, Stanford University, California.

Stuart A. L., and M. Z. Jacobson (2003), A timescale investigation of volatile chemical retention during hydrometeor freezing: Nonrime freezing and dry growth riming without spreading, *Journal of Geophysical Research*, 108(D6).

Stuart A. L., and M. Z. Jacobson (2004), Chemical retention during dry growth riming, *Journal of Geophysical Research*, 109(D07305).

Stuart A. L., and M. Z. Jacobson (2006), A numerical model of the partitioning of trace chemical solutes during drop freezing, *Journal of Atmospheric Chemistry*, 53(1), 13-42.

Telford J. W. (1996), Clouds with turbulence; the role of entrainment, *Atmospheric Research*, 40(2-4), 261-282.

Thwaites S., J. N. Carras, and W. C. McKlin (1977), The aerodynamics of oblate hailstones, *Quarterly Journal of the Royal Meteorological Society*, 103(438), 803-808.

Wilson S. R., K. R. Solomon, and X. Tang (2007), Changes in tropospheric composition and air quality due to stratospheric ozone depletion and climate change, *Photochemical & Photobiological Sciences* 6(3), 301-310.

Xu, and Jia-Liu (1983), Hail growth in a three-dimensional cloud model, *Journal Of Atmospheric Sciences*, 40(1), 185-203.

Yin Y., K. S. Carslaw, and D. J. Parker (2002), Redistribution of trace gases by convective clouds - mixed-phase processes, *Atmospheric Chemistry and Physics*, 2(4), 293-306.

Yin Y., K. S. Carslaw, and G. Feingold (2005), Vertical transport and processing of aerosols in a mixed-phase convective cloud and the feedback on cloud development, *The Quarterly Journal of the Royal Meteorological Society*, 131(605), 221-245.

Zhang Y., S. Kreidenweis, and G. R. Taylor (1998), The effects of clouds on aerosol and chemical species production and distribution. Part III: Aerosol model description and sensitivity analysis, *Journal of Atmospheric Science*, 55(6), 921-939.

Zheng G. and R. List (1994), Preliminary investigation of convective heat transfer of hailstone models, *Atmospheric Research*, 32(1-4), 75-83.

Appendices

Appendix A. Retention Model Calculations

Table A. Retention model calculations

Input Conditions	Symbol	Units	Input	Input	Formula	Range	Reference
Air temperature	Tair	C	-2.00E+00	-2.00E+00	input parameter	(15, -49) C	0 to -30C
	Tair	K	2.71E+02	2.71E+02			
Pressure	P	mb	8.00E+02	8.00E+02	input parameter	(265, 1013) mb	1013 mb to 200 mb
	P	atm	7.90E-01	7.90E-01			
pH			4.00E+00	4.00E+00			Try 4 to 7
H+ concentration			1.00E-04	1.00E-04			
Input trace chemical characteristics	HNO3		**HNO3**	**NH3**	Table 6.2		
Trace chemical molecular weight	MW	g/mol	6.30E+01	1.70E+01	Table 6.A.1		
Henry's law coefficient (@298 K)	H	M/atm	2.10E+05	6.20E+01	Table 6.A.1		S&P, pg 341
1st equilibrium constant at 298K	K_1	M	1.54E+01	1.70E-05	Table 6.3		S&P, Pg 391
2nd equilibrium constant at 298K	K_2	M	0.00E+00	0.00E+00	Table 6.4		S&P, Pg 391
Enthalpy of dissolution for Henry's Law Coefficient	ΔH	kcal/mol		-8.17E+00	Table 6.4		S&P, pg 342
Enthaply of 1st Equilibrium	DH_1eq	kcal/mol	-1.73E+01	8.65E+00	$=Ha(T1)\exp[\Delta Ha/R(1/T1-1/T2)]$		S&P, pg 345
Enthalpy of 2nd Equilibriium	DH_2eq	kcal/mol	0.00E+00	0.00E+00	$=K298\exp[-\Delta H/R(T-1-298-1)]$		S&P, pg 345
Henry's law coefficient @ freezing temp	H_A	M/atm	2.10E+05	2.18E+02	"		Eq 6.5
1st equilibrium constant at eq. freezing temp.	K_1	M	2.19E+02	4.50E-06	input parameter		temperature depenendence of K from Appendix 6
2nd equilibrium constant at eq. freezing temp.	K_2	M	0.00E+00	0.00E+00			"
Water equilibrium constant @ 298K	K_w	M	1.00E-14	1.00E-14	(1+Ka1/[H+] + Ka1Ka2/[H+]2)		
Enthalphy of water equilibrium	D_{Hw}	kcal/mol	1.34E+01	1.34E+01	HA(1+Ka1/[H+] + Ka1Ka2/[H+]2)		
Water equilibrium constant @To	K_w	M	1.29E-15	1.29E-15	K_H*RT_o		
Dissociation factor			2.19E+06	3.50E+05			

Appendix A. Continued

Table A. Continued

Input Conditions	Symbol	Units	Input	Input	Formula	Range	Reference
Overall Henry's constant	K_H*	M/atm	4.60E+11	7.61E+07			as follows form S&P, Eq 6.24, p346
Dimensionless Henry's Constant	H*	Cwtr/Cair	1.03E+13	1.71E+09	input parameter	10^4 - 10^{16}	
Effective ice-liq distribution coefficient	k_{eff}	[-]	1.00E-03	1.00E-03	input parameter	10^{-3} - 10^{-5}	Hobbs, 1974, pp 604
Input Drop characteristics					input parameter		
Cloud liquid water content	ω	g/m3	3.00E+00	3.00E+00		(0.3, 5) g/cm3	Borovikov et al., 1963, Pruppacher & Klett,
		g/cm3	3.00E-06	3.00E-06			
Drop radius (mean volume)	a	μm	5.00E+00	5.00E+00		(5, 100) mm	Jacobson, 2005. Tab 13.1, p. 447
	a	mm	5.00E-03	5.00E-03			
	a	cm	5.00E-04	5.00E-04			
Mean volume diameter	Dd	mm	1.00E+01	1.00E+01	input parameter		
	Dd	cm	1.00E-03	1.00E-03	input parameter		
Input Hail Characteristics					input parameter		
(Mass fraction) liquid water content of hail	η	-	5.00E-01	5.00E-01		(1e-4,0.5)	Lesins and List, 1986
Ice substrate temperature	Tice	C	-2.00E+00	-2.00E+00			Varies between 0 and -20
Hail diameter	Dh	mm	2.00E+00	2.00E+00		1 to 50 mm	Prupaccher & Klett, 1997
		mm	2.00E+03	2.00E+03	input parameter: for cylinder=pi; for sphere = 4		
		cm	2.00E-01	2.00E-01	input paramter		
Hail radius	r	cm	1.00E-01	1.00E-01	input parameter		
Shape factor in equation	F		4.00E+00	4.00E+00		(3.14,4)	Macklin and Payne, 1967; Jayaranthe, 1993
Collection efficiency	E		1.00E+00	1.00E+00		1.00	Lin et al., 1983

Appendix A. Continued

Table A. Continued

Input Conditions	Symbol	Units	Input	Input	Formula	Range	Reference
Super-cooled delta temp of ice-liq interface	ΔT_{int}	°C	2.00E+00	2.00E+00	vt drop, calculated below	(0,Tair)	Hobbs, 1974, pp 604 - 605, Pruppacher and Kett, 1998,
					vt hail, calculated below		
Ventilation Characteristics					=vt hail - vt drop		
Air velocity over drop	u_d	cm/s	3.25E-01	3.25E-01			Jacobson Eq 20.9 pg. 664
Air velocity over hiail	u_a-s	cm/s	6.91E+02	6.91E+02			Jacobson Eq 20.9 pg. 664
Impact speed	u_i	cm/s	6.91E+02	6.91E+02	constant		
					constant		
Constants					constant		
Universal gas constant	R	Latm/mol K	8.21E-02	8.21E-02	constant (hPa=mb)		Jac. Appendix Table A10, pg 712
Universal gas constant	R	cal/mol/K	1.99E+00	1.99E+00	constant		Jac. Appendix Table A10, pg 712
Universal gas constant	R	g/cm2/s2/mol/K	8.31E+07	8.31E+07	constant		Jac. Appendix Table A10, pg 712
Universal gas constant	R	cm3mb/mol/K	8.31E+04	8.31E+04	constant		Jac. Appendix Table A10, pg 712
Gas constant for water vapor	Rv	cm3mb/g/K	4.61E+03	4.61E+03	constant		Jac. Appendix Table A10, pg 712
Gas constant for dry air	Rdry	cm3mb/g/K	2.87E+03	2.87E+03	constant		Jac. Appendix Table A10, pg 712
Gas constant for dry air	Rdry	J/g/K	2.87E-01	2.87E-01	constant		Jac. Appendix Table A10, pg 712
Avogadros number	A	molec./mol	6.02E+23	6.02E+23	constant		Jac. Appendix Table A10, pg 711
Boltzmann constant	k	g cm2/s2/K	1.38E-16	1.38E-16			Jac. Appendix Table A10, pg 711
Gravitational acceleration	g	m/s2	9.83E+00	9.83E+00	--		Jac. Appendix Table A10, pg 711
	g	cm/s2	9.83E+02	9.83E+02			Jac. Appendix Table A10, pg 711
Properties of H2O phase change					Eq 2.55, f(Tinf)		
Equilibrium freezing temperature	To	C	0.00E+00	0.00E+00	Eq 2.56, f(Tinf)		
Equilibrium freezing temperature	To	K	2.73E+02	2.73E+02	L_s-L_m		
Latent heat of fusion at To	Lm	cal/g	7.97E+01	7.97E+01	Eq 2.62, f(Tair)		Jac, p. 40 (2nd ed)
Latent heat of ice sublimation at To	Ls	cal/g	6.77E+02	6.77E+02	"		Jac, p. 40 (2nd ed)
Latent heat of water evaporation at To	Lv	cal/g	5.98E+02	5.98E+02	n/V=P/RvTa		

Appendix A. Continued

Table A. Continued

Input Conditions	Symbol	Units	Input	Input	Formula	Range	Reference
Saturation vapor pressure over liquid at air temperature	Psat_a	mbar	5.28E+00	5.28E+00	n/V = P/RvTw		Jac, p 41
Saturation vapor pressure over liquid at To	Psat_w	mbar	6.11E+00	6.11E+00	"		"
Saturation vapor density over liquid at Tair	r_{air}	g/cm3	4.22E-06	4.22E-06	Eq 2.64 /$R_v(T_{inf+a})$		assume atmosphere is saturated w/ respect to water
Saturation vapor density over liquid at To	$r_{sat,w}$	g/cm3	4.85E-06	4.85E-06	Eq 14.19, f(Tair)		
Ice sat vapor density at Tair	$r_{sat,i}$	g/cm3	4.14E-06	4.14E-06			"
Ice sat vapor density at To	$r_{sat,i}$	g/cm3	4.85E-06	4.85E-06			Jac, p 43
Water-air surface tension	$s_{w/a}$	dyn/cm	7.59E+01	7.59E+01	Eq 4.54, f(Tair)		Jac, p 485
					Table 4.1, f(Tair)		
Properties of dry air					Eq 2.5, f(Tair)		
Dynamic viscoscity of dry air	h_{drya}	g/cm/s	1.71E-04	1.71E-04			Jac, p 102
Heat capacity of dry air at constant pressure	Cp,da	cal/g/C	2.39E-01	2.39E-01			Smith and Vanness, p 109
Thermal conductivity of dry air	ka	cal/cm/s/C	5.65E-05	5.65E-05	calculated above		Jac, p. 20
					$\varepsilon p_v/(p_a-p_v)$		
Properties of moist air					$R_{dry}(1+0.0608q_v)$		
Density of water vapor in air	rair	g/cm3 air	4.22E-06	4.22E-06	$=R/R_m$		
Mass mixing ratio of water vapor in air	w_v	g/g	4.13E-03	4.13E-03	$=P_a/R_mT$		Eq 2.31
Gas constant for moist air	Rm	cm3mb/g/K	2.88E+03	2.88E+03			Eq 2.37
Molecular weight of moist air	Ma	g/mol	2.89E+01	2.89E+01	ha/p_a		Eq 2.26
Density of moist air	ra	g/cm3	1.03E-03	1.03E-03			Eq 2.36
Dynamic viscoscity of moist air	ha	g/cm/s	1.71E-04	1.71E-04			calculated above
Kinematic viscoscity of moist air	na	cm2/s	1.67E-01	1.67E-01	r_v/R_vT_a		definition
Mean free path of moist air	la	cm	7.47E-06	7.47E-06			Eq 8.6

Appendix A. Continued

Table A. Continued

Input Conditions	Symbol	Units	Input	Input	Formula	Range	Reference
Heat capacity of moist air at constant pressure	Cp,ma	cal/g/C	2.40E-01	2.40E-01			
Partial pressure of water vapour in air	Pair	mbar	5.28E+00	5.28E+00	$= 0.211(T/To)^{1.94}(Po/P)$		Eq 2.27
Properties of water vapor							
Diffusivity of water vapor in air	Dv	cm2/s	2.63E-01	2.63E-01	calculated above		Eq. 13-3
Properties of liquid water in supercooled drop					$= (n=0, n=6\ \sum a_n T^n$		
Supercooled drop temperature	Tw_s	C	-2.00E+00	-2.00E+00	$=(n=0, n=4\ \sum anTn)$		
Supercooled drop temperature	Tw	K	2.71E+02	2.71E+02			
Density of supercooledwater	rw	g/cm3	1.00E+00	1.00E+00			Eq 3-14
Heat capacity of water	cw	cal/g/C	1.01E+00	1.01E+00	calculated above		Eq 3-16
					calculated above		
Properties of hail liquid water (during freezing (at 0C))					$= (n=0, n=6\ \sum a_n T^n$		
Water temp.	Tw	C	0.00E+00	0.00E+00	calculated above		
Water temp.	Tw	K	2.73E+02	2.73E+02			
Density of water	rw	g/cm3	1.00E+00	1.00E+00			P&K p. 87
Saturation vapor density above liquid	rsat,w	g/cm3	4.85E-06	4.85E-06	calculated above		
Properties of ice substrate							
temperature of ice substrate	Td	C	-2.00E+00	-2.00E+00			
temperature of ice substrate		K	2.71E+02	2.71E+02	input paramter		
					kv (DT)c		
Properties of Bulk Hail							
Density of Hail (Calculated)	ρ_h	g/cm3	9.57E-01	9.57E-01			0.1 (Heymsfield) to 1 g/cm3
Intrinsic ice growth velocity		cm/s	1.20E+00	1.20E+00			

Appendix A. Continued

Table A. Continued

Input Conditions	Symbol	Units	Input	Input	Formula	Range	Reference
Caculation of hail density - problematic, need to explore							
Y = $-av_{imp}/Ts$		u m/sC	1.73E+01	1.73E+01			
Bulk density of rimed ice		g/cm3	1.05E+00	1.05E+00	Heymsfield parameterization		P&K, p 661;
Bulk density of rimed ice (for compare only)		g/cm3	1.18E+00	1.18E+00	0.11(-B)^0.76		P&K, p 661; Macklin and Payne, 1962(p 41)
Density of pure ice		g/cm3	9.17E-01	9.17E-01	Eq 3-2, f(Tice)		P&K, p79
Denisty of hail (calculated)		g/cm3	9.57E-01	9.57E-01	((h/rwtr + (1 -h)/rice)^-1		weighted reciprical average
Terminal Fall Velocitiy Calculations							
For Hail Partice							
Schmidt Number	Sc	-	6.32E-01	6.32E-01	υa/Dp		eq 16.25
Knudsen Number	Kn	-	7.47E-05	7.47E-05	λ_a/r_i		eq 15.23
Bond Number	N_{Bo}	-	4.95E-01	4.95E-01			eq 20.8
Physical property number	N_P	-	5.75E+11	5.75E+11			eq 20.8
X for polynomial fit	X	-	1.28E+01	1.28E+01			eq 20.7
Y for polynomial fit	Y	-	4.10E+00	4.10E+00			"
Cunningham Slip -flow Correction factor	G	-	1.00E+00	1.00E+00	=1+Kn[A+Bexp(-C/Kn)]		eq 15 .30
Initial Termial Fall Speed (slip flow)	V^{est}	cm/s	1.22E+04	1.22E+04			eq 20.4
Initial Reynolds Number (slip Flow)	Re^{est}	-	1.47E+04	1.47E+04			eq 20.5
Reynolds Numbers Regimes							
Reynods Number- Slip Flow		-	1.47E+04	1.47E+04			eq 20.6
Reynolds Nnmber Continiuum (sphere)		-	7.47E+02	7.47E+02			eq 20.6
Reynolds Number Continuum (non-spherical)		-	8.30E+02	8.30E+02			eq 20.6
Final Reynolds Number (Hail particle)	Re^{final}	-	8.30E+02	8.30E+02			eq 20.6
Final Fall Speed (Hail particle)	V^{final}	cm/s	6.91E+02	6.91E+02			eq 29.9

Appendix A. Continued

Table A. Continued

Input Conditions	Symbol	Units	Input	Input	Formula	Range	Reference
For Drop							
Schmidt Number	Sc	-	6.32E-01	6.32E-01			eq 16.25
Knudsen Number	Kn	-	1.49E-02	1.49E-02			eq 15.23
Bond Number	N_{Bo}	-	1.29E-05	1.29E-05			eq 20.8
Physical property number	N_P	-	5.51E+11	5.51E+11			eq 20.8
X for polynomial fit	X	-	-3.08E+00	-3.08E+00			eq 20.7
Y for polynomial fit	Y	-	-6.46E+00	-6.46E+00			"
Cunningham Slip -flow Correction factor	G	-	1.02E+00	1.02E+00			eq 15 .30
Initial Termial Fall Speed (slip flow)	V^{est}	cm/s	3.25E-01	3.25E-01			eq 20.4
Initial Reynolds Number (slip Flow)	Re^{est}	-	1.95E-03	1.95E-03			eq 20.5
Reynolds Numbers Regimes							
Reynods Number- Slip Flow		-	1.95E-03	1.95E-03			eq 20.6
Reynolds Nnmber Continiuum (sphere)		-	1.86E-03	1.86E-03			eq 20.6
Reynolds Number Continuum (non-spherical)		-	2.74E-161	2.74E-161			eq 20.6
Final Reynolds Number (drop)	Re^{final}	-	1.95E-03	1.95E-03			eq 20.6
Final Fall Speed (drop)	V^{final}	cm/s	3.25E-01	3.25E-01			eq 29.9
Turbulent enhancement to heat and water vapor transfer from hail							
Gas Phase							
Prandtl number (molecular mom./heat transfer)	Pr		7.25E-01	7.25E-01	$\eta_a Cp/k_a$		Eq 16.32
Schmidt number (water vapor)	Sc_v		6.32E-01	6.32E-01	$\upsilon a/D_v$		Eq 16.25
Stokes Number w/o Cd	Ns		2.25E+00	2.25E+00	$r_w U D_d^2 / 9 m_a D_s$		Eq 4-11
$24/C_D Re$ for drop			1.00E+00	1.00E+00			Eq 8.32

Appendix A. Continued

Table A. Continued

Input Conditions	Symbol	Units	Input	Input	Formula	Range	Reference
Stokes Number w Cd	Ns		2.25E+00	2.25E+00	=Ns 24/C_DRe		after P&K, p 573 and S&P, p. 487,465
Nusselt No - smooth cylinder (Avila)	Nu_o		1.30E+01	1.30E+01	c $Re^m Pr^n$		Incopera and Dewitt, 1996, p.345, Eqn 7.47
Nusselt No - smooth cylinder(Incopera)			1.47E+01	1.47E+01	for smooth cylinder		Incopera and Dewitt, 1996, p.345, Eqn 7.47
Nusselt No (heat) - riming cylinder	Nu		2.55E+01	2.55E+01			Eqn 9
Sherwood No (water vapor) - smooth	Sh_o_v		1.24E+01	1.24E+01	like Nu		Eqn 5
Sherwood No (water vapor)- riming	Sh_v		2.43E+01	2.43E+01			Eqn 9
Ventilation coeff (water vapor)	f	-	1.21E+01	1.21E+01	Sh/2		
Determination of Schumann-Ludlam limit for wet vs dry growth							
Efficiency of collection	E		1.00E+00	1.00E+00			same as Lin et al., 1
Shape factor in equation	F		4.00E+00	4.00E+00			For clyindr = pi ; For a sphere = 4
Critical liquid water content	W_c	g/cm3	2.09E-06	2.09E-06			heat balance, Ts=0
Critical liquid water content	W_c	g/m3	2.09E+00	2.09E+00			
Growth regime			Wet	Wet	$=\pi r^2 v\omega$* eff collection $=4\pi r DF(Psat/RTh - Pa/RTa)$		
Water mass rates							
Mass rate of drop accretion	F	g/s	6.51E-05	6.51E-05			
Mass Rate of water Evaporation	E	g/s	2.53E-06	2.53E-06			
Intrinsic ice growth		g/s	1.44E-01	1.44E-01	$=4\pi r^2 Kv(\Delta tint)^c r_{ice}$		
Allowable ice growth		g/s	3.13E-05	3.13E-05	$=\eta/(1-\eta)$*Gm		
Mass rate of ice crystal growth	G_m	g/s	3.13E-05	3.13E-05	=Gm + Lw		Eq 6.17 (Stuart 2000, PhD Dissertation, p135)
Mass rate of change of liquid water in hail	L_w	g/s	3.13E-05	3.13E-05			assumes constant liquid water content in hail
Mass Growth rate	G	g/s	6.26E-05	6.26E-05			derived from initial model equation.
Mass Growth check			6.26E-05	6.26E-05			
Mass Rate of Drop Shedding	S	g/s	0.00E+00	0.00E+00	F-E-G		assumes constant liquid water content in hail

Appendix A. Continued

Table A. Continued

Input Conditions	Symbol	Units	Input	Input	Formula	Range	Reference
Calculation of Retention							
keff			1.00E-03	1.00E-03			
1-keff			9.99E-01	9.99E-01			
h			5.00E-01	5.00E-01			
1-h			5.00E-01	5.00E-01			
1/H*		Cair/Cwtr	9.69E-14	5.86E-10			
rL		g/cm3	1.00E+00	1.00E+00			
rVLsat		g/cm3	4.85E-06	4.85E-06			
rL / rlVsat			2.06E+05	2.06E+05			
n	G/F		9.61E-01	9.61E-01			
m	E/F		3.88E-02	3.88E-02			
numerator							
h + keff (1-h)			5.01E-01	5.01E-01			
denominator							
1-n-m (shedding effect)			-1.04E-16	-1.04E-16			
n(h+keff(1-h)) (growth effect)			4.81E-01	4.81E-01			
m(1/H*rL / rvl) (evaporation effect)			7.75E-10	4.69E-06			
total denominator			4.81E-01	4.81E-01			
Retention ratio	Γ	-	1.04E+00	1.04E+00		$=h+k_e(1-h) / 1-[1-h-k_e(1-)]n-[(1-1/H*(r_L / r_{vl}^{sat})]m$	
Mass Balance Testing							
Water Mass Balance Check		g/s	0.00E+00	0.00E+00			Should be zero
Solute mass balance							
Average mixing ratio of chemical in air		pptv	5.00E+01	5.00E+01			Seinfeld & Pandis, pg 61
	Ca	g/cm3	1.12E-13	3.02E-14	=pptv/1e12*P/RT*MW		

Appendix A. Continued

Table A. Continued

Input Conditions	Symbol	Units	Input	Input	Formula	Range	Reference
solute mass fraction_drop	Xd	g_chem/g_wtr	1.15E+00	5.15E-05	$=Ca*H/r_{wtr}$		
solute mass fraction_hail	Xh	g_chem/g_wtr	1.20E+00	5.36E-05	$=GX_d$		
solute mass fraction_shed liquid	Xl	g_chem/g_wtr	2.40E+00	1.07E-04	$=X_h/(h+keff(1-h)$		
solute mass fraction_evap sol'n	Xe	g_chem/g_wtr	4.79E-08	1.29E-08	=Xl*(1/H)*(rl/rvlsat)		
solute mass in via accretion	Xd*F	g_chem/s	7.52E-05	3.35E-09			
solute mass out via shedding	Xl*S	g_chem/s	0.00E+00	0.00E+00			
solute mass out via evaporation	Xe*E	g_chem/s	1.21E-13	3.27E-14			
solute mass accumulation in hail	Xh*G	g_chem/s	7.52E-05	3.35E-09			
solute mass balance check	check	g_chem/s	0.00E+00	0.00E+00			should be zero
retention check			1.04E+00	1.04E+00			

About the Author

Ryan Algernon Michael was born in New Amsterdam, Guyana. He completed his undergraduate degree at the University of Guyana during the fall of 2005, majoring in chemistry, with biology minor. He graduated with honors, and as awarded the Dean's Award for the Best Graduating Chemistry Student, as well as the University of Guyana Award for the Best Graduating Natural Science Student. He worked briefly at Berger Paints, Barbados Ltd, in the Quality Control Department for paint production. Ryan received a Master of Engineering Sciences degree from the University of South Florida in the fall of 2008.